LAWRENCE
LIVERMORE
NATIONAL
LABORATORY

LLNL-JRNL-668947

Fighting Ebola through Novel Decontamination Technologies for the Military

C. J. Doona, F. E. Feeherry, K. Kustin, G. G. Olinger, P. Setlow, A. J. Malkin, T. Leighton

March 24, 2015

Frontiers in Microbiology

Disclaimer

Frontiers in Microbiology

Research Topic: Microbial Decontamination by Novel Technologies – Analytic Approaches and Mechanistic Insights

(Henry Jaeger, Alexander Mathys, Kai Reineke, Eds)

Fighting Ebola through Novel Decontamination Technologies for the Military

[1]Christopher J. Doona[*], [1]Florence E. Feeherry, [2]Kenneth Kustin, [3]Gene G. Olinger, [4]Peter Setlow, [5]Alexander J. Malkin, [6]Terrance Leighton

[*]Correspondence to: Christopher J. Doona at christopher.j.doona.civ@mail.mil

[1]United States Army-Natick Soldier RD&E Center

Warfighter Directorate

RDNS-SEW-TMM

Kansas St

Natick, MA 01760-5018

[2]Department of Chemistry, *Emeritus*

Brandeis University MS015

Waltham, MA 02254-9110

[3]National Institute of Allergy and Infectious Diseases (NIAID)

Integrated Research Facility - Division of Clinical Research

Office 1A-120

8200 Research Plaza

Fort Detrick, MD 21702

[4]Department of Molecular Biology and Biophysics

University of Connecticut Health Center

263 Farmington Avenue

Farmington, CT 06030-3305

[5]Biosciences and Biotechnology Division

Physical and Life Sciences Directorate

Lawrence Livermore National Laboratory

Mail-stop 233

P.O. Box 808, 7000 East Ave

Livermore, CA 94551

[6]UCSF Benioff

Children's Hospital Oakland Research Institute

5700 Martin Luther King Jr. Way

Oakland, CA 94609

Abstract

Recently, global public health organizations such as Doctors without Borders (MSF), the World Health Organization (WHO), Public Health Canada, National Institutes of Health (NIH), and the U.S. government have deployed Field Decontamination Kits for the sterilization of Ebola-contaminated medical devices at remote clinical sites in crisis-stricken regions of West Africa (medical waste materials are placed in bags and burned). The basis for effectuating sterilization is chlorine dioxide (ClO_2) produced by novel decontamination technologies that were invented by researchers at the US Army – Natick Soldier RD&E Center (NSRDEC). In fact, research scientists at NSRDEC invented an ensemble of dry-mix chemical decontamination technologies designed for various decontamination applications involving fresh produce; food contact and handling surfaces; personal protective equipment; textiles used in clothing, uniforms, tents, and shelters; graywater recycling; airplanes; surgical instruments; and hard surfaces in latrines, laundries, and deployable medical facilities. These examples demonstrate the far-reaching impact, adaptability, and versatility of innovative nonthermal processing technologies for the pasteurization and sterilization of foodstuffs that extend into other technical areas. We present herein the unique attributes of NSRDECs novel decontamination technologies and a Case Study of the development of Field Decontamination Kits for sterilizing Ebola-contaminated medical equipment in the field by global public health organizations in West Africa. We also review mechanisms of bacterial spore inactivation by novel, emerging, and established nonthermal technologies for food preservation, such as high pressure processing, irradiation, cold plasma, and chemical sanitizers, using an array of *Bacillus subtilis* mutants to probe mechanisms of spore

germination and inactivation. Further, we employ techniques of high-resolution Atomic Force Microscopy and phase contrast microscopy to examine effects of γ-irradiation on bacterial spores (e.g., *Bacillus anthracis*, *Bacillus thuringiensis*, and *Bacillus atrophaeus spp.*) and of chlorine dioxide on *B. subtilis* spores, and assays using spore bio-indicators to ensure sterility when decontaminating with chlorine dioxide.

Introduction

Innovation in Science and Technology comes from myriad sources, such as thinking outside-the-box, applying expertise to new areas, or adapting novel technologies that advance the frontiers of knowledge to fill critical capability gaps on the battlefield and needs in the commercial marketplace for consumers. Since the time when chlorine dioxide (ClO_2) was used to decontaminate *Bacillus anthracis* spores (causative agent of 'Anthrax') during the attacks on Washington, DC, researchers at the U.S. Army − Natick Soldier Research, Development and Engineering Center (NSRDEC) have invented and patented (Doona et al., 2014) an ensemble of novel decontamination technologies (Table 1) involving innovative methods and unique apparatuses for generating ClO_2. These dry, mixed-chemical technologies are lightweight, compact, portable, energy-independent, flameless, inexpensive, safe to end-users and the environment ("green" technologies), and use low volumes of water to address a diverse array of decontamination applications in far-forward military deployments or other austere environments, such as those that occur during emergencies, natural disasters (Hurricane Katrina, tsunamis, superstorm Sandy) or in humanitarian relief in third-world countries. Thus, when the Ebola crisis erupted in the summer of 2014, global public health and medical personnel adapted NSRDEC's novel decontamination technologies for field use to fight the spread of Ebola by decontaminating medical equipment at remote clinical sites in West Africa.

Ebola virus disease (EVD) is a severe and often fatal disease in humans that is communicated between humans through contact with infected blood, organs or tissues, bodily fluids (saliva, sweat, vomit, urine, semen, and breast milk), or items they contaminate (clothing, bedding,

gauze, needles and syringes, and medical equipment). In October, 2014, WHO estimated 10,141 cases and 4922 deaths from this outbreak, and concerns of EVD heightened as EVD cases spread internationally. As an enveloped virus – one with a lipid and protein membrane – Ebola is vulnerable to chemical disinfectants, such as household bleach (OCl^-) and chlorine dioxide (ClO_2), which can be used to sanitize infected surfaces, patient rooms, and to sterilize contaminated medical equipment at remote clinical sites in West Africa (WHO, 2014). In parts of the world that consume non-traditional foods (bats, monkeys, bush meat) as protein sources, basic food hygiene for preventing the transmission of biological hazards apply equally well to the Ebola virus (Anelich and Moy, 2014; WHO, 2015): Keep clean, Separate raw and cooked, Cook thoroughly (specifically, boiling for 5 min or heating for 60 min at T = 60 °C inactivates the Ebola virus – Anelich and Moy, 2014), Keep food at safe temperatures, Use safe water and raw materials.

NSRDEC's ensemble of patented novel decontamination technologies have the acronyms NCC, PCS, D-FENS, D-FEND ALL, and CoD (Table 1) and feature a variety of embodiments to produce ClO_2 for killing bacterial spores (*B. anthracis*), vegetative pathogens (*Listeria monocytogenes*, *Escherichia coli*, etc.,), viruses (Ebola), and bacteriophage in cross-cutting applications (Setlow et al., 2009), such as sterilizing surgical instruments, decontaminating textiles (uniforms, tents, shelters), sanitizing fresh fruits and vegetables procured in host nations, disinfecting wastewater and improving potable water quality and safety, and promoting hygiene by decontaminating surfaces bathrooms, showers, laundries, Army Field Kitchens, Navy Galleys, and deployable medical units. Deployments of military personnel worldwide generate thousands of tons of wastewater and food waste annually that support disease vectors capable of

adversely affecting human health and account for Disease and Non-Battle Injuries (DNBIs) at an average rate of 1.5% of assigned personnel, which cost the Army $32.5M annually (300 soldiers per day) during the time of the Balkan conflicts in the 1990s! Finding inexpensive, convenient, and effective decontamination technologies improves hygiene and reduces the incidences of DNBIs and other foodborne illnesses, thereby saving all branches of the military many dollars in medical costs and promoting health and well-being. In 2012, Thomson Reuters named the U.S. Army among the Top 100 Global Innovators for innovative patents such as these (Foran, 2013 − available at http://www.army.mil/article/99816/, accessed 12 March 2015). Other technologies that decontaminate with gaseous ClO_2 include electrically-powered equipment to decontaminate facemasks (Personal Protective Equipment, PPE, worn by emergency first-responders − Stubblefield and Newsome, 2015), and Field Decontamination Kits (FDKs) based on the commercial-off-the-shelf (COTS) version of NRDEC's decontamination technologies, that are presently being used by global public health organizations (Doctors without Borders, MSF, World Health Organization, WHO, Public Health Canada, National Institutes of Health, NIH) and the U.S. government to sterilize Ebola-contaminated medical equipment at remote clinical sites in West Africa.

We focus herein primarily on NSRDEC's novel decontamination technologies and the mechanisms through which ClO_2 inactivates bacterial spores, with spores being the most resistant class of microorganisms and commonly used as indicators of sterility and/or decontamination efficacy. We explore the characteristics and validation of these decontamination technologies, with particular emphasis on the field use of these inventions in FDKs to aid in the fight against the spread of Ebola. While Nonthermal food processing technologies (chemical

sanitizers, high pressure, irradiation, heat, plasmas, and UV light) primarily attempt to inactivate vegetative pathogens or *Clostridium botulinum* spores in low-acid foods, many of these lethal agents, particularly high pressure, have also been used in the decontamination of *B. anthracis* (Cléry-Barraud et al., 2004) or other types of spores, and we also consider the mechanisms of bacterial spore inactivation by these agents. The ability of ClO_2 to kill spores used as bio-indicators of sterility is also examined in detail.

1.0 NSRDEC's novel decontamination technologies

Chlorine dioxide (ClO_2) is a versatile disinfectant that is readily adapted for use in novel technologies (NCC, PCS, D-FENS, D-FEND ALL, CoD, FDKs) for numerous decontamination applications. In the NCC (Table 1), ClO_2 is generated through unique chemical processes that improve the generation of ClO_2 compared to existing methods, which include *i*) the reduction of chlorate [ClO_3^-, Cl(V)] in high acid (HCl or H_2SO_4); *ii*) the oxidation of chlorite [ClO_2^-, Cl(III)] by dichlorine [Cl_2, Cl(0)], hypochlorite [OCl^-, Cl(I)], or persulfate [$S_2O_8^{2-}$, S(VII)], or *iii*) the acidification of chlorite for the formation and subsequent disproportionation of chlorous acid [$HClO_2$, Cl(III)] (Horváth et al., 2003). The NCC generates chlorine dioxide by the reduction of chlorite through the use of a unique chemical effector (Curtin et al., 2004) that initiates and controls the reaction rate and the production of chlorine dioxide such that the reaction takes place at near-neutral pH on a practical and relatively short timescale (Curtin et al., 2014) – it is sold commercially as a COTS product that occurred in part as a result of Technology Transfer licensing agreements with private industry.

The PCS (Figure 1) is a Modern Field Autoclave, a revolutionary medical device invented to meet a stated Army need and an urgent battlefield demand for a field-portable, non-steam sterilizer technology that can be used by far-forward surgical teams (Doona et al., 2014). The PCS produces gaseous ClO_2 and proceeds where no commercial device existed previously, with a 100% reduction in power usage, 98% reduction in water, 95% reduction in weight, and 96% reduction in cubic footprint compared to conventional steam autoclaves. D-FENS (Figure 2) generates aqueous chlorine dioxide in a collapsible handheld spray bottle (Doona et al., 2014) for decontaminating surfaces (fresh produce or medical, food handling, and surfaces in showers and latrines) anywhere large numbers of deployed personnel co-exist in close proximity. D-FEND ALL and CoD eliminate the effector in generating ClO_2 and provide more convenience in treating water, decontaminating textiles, or for in-package anti-microbial treatments of sterile instruments or fresh fruits and vegetables. FDKs are based on adapting commercial versions of the NSRDEC decontamination technologies for use by global public health organizations (MSF, WHO, NIH, etc.) to sterilize Ebola-contaminated medical equipment at remote clinical sites in West Africa.

1.1 Field Decontamination Kits in the Ebola crisis

Emerging and re-emerging viral infectious diseases have been identified as a major threat to human health, and the current outbreak of EVD has impacted a large part of western Africa. Conventional procedures for the decontamination of equipment during a filovirus outbreak rely on the use of chemical chlorine (bleach, aqueous hypochlorite, OCl^-) for decontamination when exiting an isolation/treatment center. Electrical equipment that enters an isolation/treatment center and diagnostic facilities can only be surface decontaminated by aqueous rinses with 0.5 −

5.0% chlorine bleach solution (household bleach is about 6% OCl^-). This procedure is likely *not* adequate for complete decontamination of the devices, particularly for accessing inside the devices.

Devices such as personal cell phones, computers, and most importantly, expensive medical point-of-care (POC) electronic devices used for clinical assessment of patients in isolation/treatment wards are not sufficiently decontaminated by surface rinses. Some medical diagnostic devices have closed systems internal to the device that may have infrequent but probable contamination that cannot be adequately decontaminated by surface rinses with a chemical decontaminating agent. Often these devices contain valuable internal components that may be recycled after being surface decontaminated. This is extremely problematic for items used in a high hazard environment. For low resource, remote sites, the deployment of traditional decontamination tools is nearly impossible. Often there is limited space for equipment, so another desirable aspect of the FDK method is its compact size and simple disposal routine post-decontamination cycle.

Given the wide use of and acceptability of chlorine bleach solutions in laboratories and in isolation/treatment centers, and the historical use of chlorine dioxide in the decontamination of equipment in the U.S., we decided to adapt a chlorine dioxide method to provide equipment decontamination for deployment in the field in areas of active outbreak. This safe and adaptable method uses a commercially available COTS packaged chemical combination kit in which the components are packaged separately and isolated from water to prevent chemical reaction from taking place. Once mixed together with water, the chemical reduction of sodium chlorite initiates

within minutes, and a well-controlled, exothermic reaction takes place that releases chlorine dioxide gas from solution. This reaction is carefully designed to occur inside a closable plastic bag, such that the ClO_2 released decontaminates thoroughly the entire interior volume of the bag and all items contained therein, including permeating the interior regions of the electronic medical and other devices inside the decontamination bag. Humidity and mild heat and mild pressure accumulate inside the bag from the chemical reaction occurring inside a closed container, but the heat and pressure gently subside over the 30-60 minute decontamination period. Human exposure to ClO_2 above permissible concentrations and durations is known to cause irritation of the eyes, skin, nose, throat and lungs, and thus this method is typically used in outdoor environments with exposure to the sun.

Adapting this method for field decontamination was ideal, because it is devoid of electrical power sources, uses small quantities of water form available sources, and the low cost of the Field Decotnamination Kits (FDKs), and with the required supplies simple and easy to obtain, store, and handle for ClO_2 generation. Specifically, this method was used to develop FDKs (Table 1, Figure 3) comprising a self-sealable bag (2 or 10 gallon capacity), dry chemical components (Part A and Part B) available commercially as a kit that react in water to produce chlorine dioxide. The FDK also includes a device to measure water (50 mL tube) and chlorine dioxide indicators of sterility. In addition, laboratory testing with spore biological indicators (discussed below in Section 4.0) showed complete inactivation of spores (sterility) was achieved within 30 minutes of exposure.

Figure 3 illustrates the procedural steps carried out in utilizing the FDKs. Briefly, the ClO_2 indicators are taped to the inner bag to be observed during the decontamination process and the chemical reagents Part A and Part B are placed in a container with water. The item to be decontaminated is placed in the bag near or over the mixture and the bag is subsequently sealed. Within a few minutes the reaction produces condensation (humidity) and yellow ClO_2 gas that inflates the bag due to a mild build-up of heat and of mild pressure, although the bag itself does *not* become turgid. After a minimum of 30 minutes, the color change of the indicator shows adequate concentration and exposure to ClO_2 gas to achieve sterility, and the bag can be opened to release the trapped gas. The equipment can then be removed and surface-cleaned, since the water, ClO_2, and inert salts from the spent reaction can be present on the surface. The remaining solution and materiel can be bagged and disposed of according to local policies.

More than 150 FDKs have been deployed for use by global public health organizations during the Ebola outbreaks in western Africa, which includes Guinea, Sierra Leone, and Liberia, to protect patients and health care personnel. The FDKs have been used to decontaminate laboratory equipment, POC medical devices and personal cell phones. Overall, the performance has been acceptable and only on occasion have the bags leaked gas during the sterilization cycle, thereby requiring longer exposure times to effectuate the color change of the ClO_2 indicator strip and signify exposure sufficient to ensure sterility. For the purpose of field deployment, these kits are safe, compact and easy to ship to remote sites that have limited infrastructure and resources available.

1.2 Laboratory testing NIH/NIAID Field Decontamination Kits

Instructions for the FDKs involve putting Part A and Part B together into a reaction vessel, then adding water. Independent laboratory testing showed that increasing the volume of water slightly and adding the water to the reaction vessel first, followed by adding Part A (oxidant) with stirring, then Part B (reductant) with stirring helped ensure the reaction runs controllably and smoothly, while evolving the maximum amount of ClO_2 gas. Small FDKs consist of a 2.5 gallon sealable mylar bag, 15 g of Part A, 4 g of Part B, and 30 mL of water mixed inside a 100 mL beaker as the reaction vessel. Large FDKs were scaled proportionately to consist of a 10-gallon bag, 60 g of Part A, 16 g of Part B, and 120 mL of water in a 600 mL beaker as the reactor vessel. In both configurations, the chemical reaction initiates slowly, then releases copious gaseous ClO_2 at approximately 2 min and 15 sec after all of the reagents were combined. These reaction compositions with various permutations were run inside the different FDKs (2.5- and 10-gallon bags) and also inside the PCS, using spectrophotometry to monitor [ClO_2] at $\lambda = 360$ nm (the absorbance maximum of ClO_2) and a combination probe that measures %RH and temperature simultaneously (Kalibrier-Protokoll). In addition, the reaction was monitored with ClO_2 color-change indicator strips (ClorDiSys Solutions, Inc.) and commercially available spore indicators of *Geobacillus stearothermophilus* in Tyvek (ClorDiSys Solutions, Inc), *G. stearothermophilus* for steam sterilization (BT Sure, Thermo Scientific), and *B. atrophaeus* for ethylene oxide sterilization (EZ Test, SGM Biotch, Inc). Representative results are summarized in Table 2 using the commercial chemical sets and the three different container units (2.5-gal bag, 10-gal bag, and PCS) run for 30 minutes. In all instances, the CD-CHEK strips turned color (indicative of sufficient ClO_2 exposure for sterilization) and all of the spore bio-indicators confirmed sterility had been achieved.

2.0 Bacterial spore properties –mechanisms of resistance and killing

The novel ClO_2 decontamination technologies mentioned above are laboratory inventions that were patented, commercialized, and adapted for actual field use in austere environments (e.g., far-forward military deployments or global humanitarian relief in third-world countries, etc.). In all cases, these decontamination technologies have to be validated for efficacy in the laboratory and during their actual field use. Typically this process involves using commercially available bacterial spore indicators for convenience (discussed below in Section 4.0), although live cultures could also be used. Thus, we look at the unique properties and attributes that impart bacterial spores with extreme resistance to lethal agents, and consider the underlying mechanisms of bacterial spore inactivation during decontamination by ClO_2 and other nonthermal technologies used for decontamination or food processing and preservation.

2.1 Bacterial spores – background

Members of bacteria of *Bacillus* and *Clostridium* species and their close relatives can form metabolically dormant spores, generally when the environment no longer can support growth (Setlow, 2006; Leggett et al., 2012; Setlow and Johnson, 2012). Spores are extremely resistant to all manner of harmful treatments, and can remain dormant for years. However, if given the proper stimuli, generally nutrients such as amino acids or sugars, spores can return to life in minutes and outgrow into vegetative cells (Setlow, 2013). During subsequent growth, the growing or stationary phase cells of some spore-formers can secrete toxins or deleterious enzymes, and these agents can cause food spoilage or food poisoning and other human or animal diseases. As a consequence, there is much interest in the mechanisms of spore resistance to and

the killing of spores by different treatments including high pressure, radiation, chemicals, plasma, or heat. One factor that is often overlooked in thinking about these mechanisms is the significant heterogeneity in properties of individual spores in genetically homogeneous spore populations, and this is seen in levels of spore resistance and in rates of spore germination (Setlow et al., 2012). The reasons for some of this heterogeneity are known, in particular some of the causes of the variability in rates of germination between individual spores. However, the reasons for the variability in resistance properties between individual spores in populations are not clear.

2.2 Spore structure, components, properties and their role(s)s in spore resistance

A number of novel spore structures and many spore-specific components and features are crucial for imparting various spore resistance properties (Table 3). Spores of all species appear to have a generally similar basic structure (Fig. 4), with the exception of the outermost exosporium layer that is present in spores of some species, but not all (Henriques and Moran, 2007). The large balloon-like exosporium is composed of proteins, sugars, and lipid, and it is present in many spore formers that can cause disease, including the members of the *Bacillus cereus* group and *Clostridium difficile*, but is absent from the model spore former *Bacillus subtilis*. This structure appears to be important in spore adhesion properties, and in restricting access of antibodies to the spore coat layer below the exosporium, but plays no major role in most spore resistance properties (Setlow, 2006; Henriques and Moran, 2007). The exosporium may also play some role in virulence of spores, but this role is not yet clear.

Moving from the exterior inward, the spore coat is found under the exosporium, and is composed of many spore-specific proteins assembled in a number of layers (Henriques and Moran, 2007; McKenney et al., 2013). The coat can contain up to 50% of total spore proteins, and protects more inner spore layers such as peptidoglycan from attack by lytic enzymes such as lysozyme, and also by lytic enzymes of predatory eukaryotes. The coat is also probably crucial in the resistance of spores to a variety of chemicals, including chlorine dioxide (ClO_2) and sodium hypochlorite (bleach, OCl^-), that are widely used for spore decontamination. As a consequence, spores that have defective coats because of mutation(s) or chemical de-coating are sensitized to these oxyhalogens and to many other types of chemicals, although not to all. Indeed, the coat plays only a minor role in spore resistance to chemicals such as H_2O_2, nitrous acid, acid and alkali, and DNA alkylating agents (Table 3). In a few cases, enzymes present in spore coats, superoxide dismutases (SODs catalyze the dismutation of superoxide, $O_2^{-\bullet}$, to O_2 or to H_2O_2) and catalases (catalyze the disproportionation of H_2O_2 to O_2 and H_2O), have been shown to play roles in spore resistance to some oxidizing agents, both *in vitro* and in *in vivo*-like environments (Henriques and Moran, 2007; McKenney et al., 2013; Cybulski et al., 2009).

Beneath the spore coat is found the outer membrane, which is a critical element in spore formation. While it is possible that the outer membrane is a permeability barrier in dormant spores (Gerhardt and Black, 1961; Rode et al., 1962), this role is not clear, and there are no mutants that specifically affect the spore's outer membrane. The outer membrane is also lost either partially or completely in spores with defective coats, and the outer membrane is also removed by chemical de-coating treatments (Buchanan and Neyman, 1986). In general, the outer membrane specifically is thought not to play a major role in spore resistance properties, but it is

actually difficult to separate the roles of the outer membrane and coat in determining spore resistance properties.

Under the outer membrane are two layers of peptidoglycan (PG); first, the large spore cortex, then the thinner germ cell wall that comprises the minority of total spore PG (Popham, 2002). The germ cell wall PG has a structure that appears identical to that of growing cell wall PG structure, and cortex PG has a structure similar to that of the germ cell wall PG, but with several cortex-specific modifications. As a consequence, in the process of spore germination, cortex-lytic enzymes (CLEs) degrade cortex PG, while leaving the germ cell wall intact and allowing this structure to form the cell wall of the outgrowing spore (Setlow, 2013). The cortex's main role in spore resistance appears to be to maintain and possibly help establish the extremely low water content in the central spore core (25-50% of wet wt) that is crucial in spore resistance to wet heat (Table 3) and probably in spore dormancy (see below). There are a number of *B. subtilis* mutants that affect cortex PG structure. Some changes in cortex PG are associated with changes in spore wet heat resistance, and, in some cases, changes in cortex PG are associated with changes in spore core water content (Zhang et al., 2012).

Under the germ cell wall is found the second spore membrane called the inner membrane (IM). This IM has a phospholipid and fatty acid composition similar to the plasma membrane of the growing or sporulating cell (Griffiths and Setlow, 2009). However, lipid probes in the IM are immobile, suggesting the IM is not as fluid as membranes in growing cells, although IM fluidity is restored when spores complete germination and the core expands (Cowan et al., 2004). This expansion takes place in the absence of any ATP synthesis as the volume enclosed by the IM

increases more than 2-fold. As with IM lipid mobility, IM permeability also rises dramatically, when the IM enclosed volume increases during spore germination. The low permeability of the dormant spore IM appears to contribute significantly to spore resistance to hydrophilic chemicals, as changes in dormant spore IM permeability due to changes in sporulation conditions, primarily temperature, parallel changes in IM permeability (Cortezzo and Setlow, 2004). It has been suggested that the IM is held in some sort of compressed state in the dormant spore, and this suggested structure is consistent with the extremely low permeability of the IM observed in dormant spores, even to a hydrophobic molecule such as methylamine, and perhaps even to water (Setlow and Setlow, 1980; Swerdlow et al., 1981; Cortezzo and Setlow, 2004; Sunde et al., 2009; Ghosal et al., 2010; Kaieda et al., 2013; Kong et al., 2013). Unfortunately, the precise structure of dormant spores' IM and how this structure influences IM permeability are still not clear. This is important information, because a number of key proteins in spore germination are in the IM (Setlow and Johnson, 2012; Setlow, 2013), and IM properties will most likely influence the function of these germination proteins.

The final spore layer is the central core, the site of spore DNA, RNA, and most spore enzymes. As noted above, the core has low water content, and this undoubtedly is the reason that soluble, mobile and active proteins in growing cells are immobile and inactive in the spore core (Gerhardt and Marquis, 1989; Setlow, 1994; Cowan et al., 2003). Indeed, while the dormant spore core has enzymes such as catalases and superoxide dismutases that play major roles in the resistance of growing cells to oxidizing agents, these enzymes play no role in dormant spore resistance, presumptively because they are inactive in the environment of the dormant spore core (Setlow, 2006; Leggett et al., 2012). The low core water content is most likely the major factor in spore

resistance to wet heat (Gerhardt and Marquis, 1989). There are also at least three other unique spore core features to consider. First, the core pH is ~ 1.5 units lower than the pH in a growing cell or in the mother cell compartment of the sporulating cell (Setlow and Setlow, 1980). The importance of this low core pH in spore resistance is not clear, since the core pH can be elevated 1.5 units with no effects on spore dormancy or resistance (Swerdlow et al., 1981). However, the decrease in spore core pH during sporulation appears to be important in the modulation of enzyme activity in the developing spore late in sporulation (Setlow, 1994). Enzymes that are modulated in this way include the zymogen of the GPR protease that auto-activates at a low pH, and phosphoglycerate mutase (catalyzes the interconversion of 3-phosphoglycerate, 3-PGA, to 2-phosphoglycerate) that becomes much less active at pH ~6.3, thus causing the accumulation of a large amount of 3-PGA in the dormant spore (Illades-Aguiar and Setlow, 1994; Setlow, 1994). This 3-PGA depot is rapidly catabolized to generate ATP in the first minutes of spore germination, during which core pH rises to ~7.8 and core water content rises to ~ 80% of wet wt (Setlow and Johnson, 2012; Setlow, 2013).

A second unique feature of the spore core is the high level (~ 20% of core dry wt) of pyridine-2,6-dicarboxylic acid (dipicolinic acid, DPA), which exists as a 1:1 chelate with divalent cations, predominantly Ca^{2+} (CaDPA) (Gerhardt and Marquis, 1989; Setlow, 2006; Setlow and Johnson, 2012). DPA is made in the mother cell compartment of the sporulating cell, and the accumulation of CaDPA in the core late in sporulation plays a significant role in reducing spore core water content (Paidhungat et al., 2000). CaDPA in the core also has significant affects on spore DNA photochemistry, and thus CaDPA accumulation in the core alters spore resistance to UV radiation, but actually sensitizes DNA to UV radiation at some wavelengths (Setlow, 2001;

Setlow, 2007). While the spores' huge CaDPA depot is stable for long periods in spores suspended in water even at relatively high temperatures (75 − 80 °C for *B. subtilis* spores), the spores' entire CaDPA depot is released rapidly in the first minutes of spore germination (Setlow, 2013). In addition, treatment with a number of oxidizing agents alters spores in some fashion such that their CaDPA depot is released completely even at 75 °C (Cortezzo et al., 2004).

Another notable unique feature of the spore core is the saturation of spore DNA with a group of novel small DNA-binding proteins, termed Small, Acid-Soluble Proteins (SASP) of the α/β-type, so named because the two major proteins of this type in *B. subtilis* were initially termed SASP-α and SASP-β (Setlow, 2001; Setlow, 2007). The amino acid sequences of these ~ 60-75 residue proteins are unique and extremely well conserved both within and across spore forming species, including members of both *Clostridiales* and *Bacillales*. The α/β-type SASP play major roles in protecting spore DNA against UV radiation (~ 260 nm) by changing DNA structure from the B-form to an A-like form in which the UV photoproducts formed in growing cell DNA, including cyclobutane pyrimidine dimers and 6-4 photoproducts between adjacent pyrimidines, are not generated, and some of the latter UV lesions are extremely mutagenic and thus potentially lethal. In contrast, with α/β-type SASP saturated DNA the major UV photoproduct generated by ~ 260 nm radiation is a novel thymine-thymine adduct initially called the spore photoproduct (SP), and spores have a number of enzymes that repair SP in a relatively error-free manner. Thus α/β-type SASP are a major factor in spore resistance to UV radiation and also to γ-radiation, although repair of DNA damage in spore outgrowth is also important (Setlow, 2001; Setlow, 2007; Moeller et al., 2014). The α/β-type SASP also protect spore DNA against other types of damage, particularly depurination by wet and dry heat, and also against a number of

genotoxic chemicals, including nitrous acid and formaldehyde (Setlow, 2006). The structure of a complex of an α/β-type SASP bound to a short DNA fragment in conjunction with modeling studies based on this structure have elucidated the causes of these effects of α/β-type SASP on DNA properties at the atomic level (Lee et al., 2008).

The α/β-type SASP are degraded in the first minutes of spore germination and outgrowth (Setlow, 1994; Setlow, 2013) in a process initiated by an endoprotease termed GPR that is specific for a conserved sequence found in all α/β-type SASP. Oligopeptides generated by GPR cleavage are then degraded rapidly to free amino acids that are re-utilized by the outgrowing spore for metabolism and protein synthesis. Spores in which α/β-type SASP are not degraded rapidly following spore germination, either because GPR is inactive or because an α/β-type SASP binds too tightly to DNA, exhibit slow outgrowth and in some cases decreased viability (Setlow, 1994; Hayes and Setlow, 2001).

2.3 Mechanisms of Spore Killing

Work primarily with *B. subtilis* spores, and some with spores of other species (Setlow, 2006; Setlow et al., 2014), has identified five different mechanisms for killing of spores by various agents (Table 3). These are: 1) DNA damage; 2) damage to the spores' IM; 3) damage to some essential spore core protein; 4) explosive rupture of the dormant spores' IM; and 5) destruction of one or more spore components that are essential for spore germination. It is important to note that spores apparently inactivated by the last mechanism may not actually be dead, but just cannot return to active growth, since spore germination is blocked. There are a number of examples of spores that appear dead because they can't germinate, but return to life, when

assisted in spore germination, generally by provision with a lytic enzyme that can degrade spores' PG cortex (Setlow et al., 2002; Paredes-Sabja et al., 2009a; Paredes-Sabja et al., 2009b; Burns et al., 2010). This has been observed with spores that are apparently inactivated by treatment with chemical agents that either remove and/or inactivate enzymes in spores' outer layers such as CLEs and/or proteases that can activate CLE zymogens in spores of *Clostridium* species. Thus, it is crucial to ensure that a spore killing regimen has not simply rendered spores incapable of germinating, such that the treated spores cannot be revived by artificial germination treatments; a number of tests have been used to demonstrate this (Setlow et al., 2014).

Among the other four methods of spore killing, the rarest is probably explosive rupture of the dormant spores' outer layers. This phenomenon has only been seen with spores incubated in rather high concentrations of strong mineral acids such as HCl or HNO_3 (Setlow et al., 2002; Setlow, 2006). As would be expected, UV and γ-radiation kill spores largely by DNA damage, since loss of DNA repair capacity greatly decreases spore resistance to these treatments, and survivors of these radiation treatments also accumulate high levels of mutations. A number of genotoxic chemicals, including nitrous acid and formaldehyde, also kill spores by DNA damage, as does dry heat, which generates significant levels of abasic sites in DNA. However, the potentially genotoxic agent, H_2O_2, does not kill spores by DNA damage, because of the strong protection of DNA against H_2O_2 damage by the α/β-type SASP.

Surprisingly, wet heat treatment does not kill spores by DNA damage, even though the temperatures used for spore killing, $\geq$ 90°C, might be expected to generate many abasic sites in DNA due to depurination. However, α/β-type SASP protect DNA so well against damage by

wet heat that wet heat almost certainly kills spores by damage to one or more essential core proteins (Setlow, 2006; Coleman et al., 2007; Coleman et al., 2010; Leggett et al., 2012). As might be expected, spores lacking the majority of their α/β-type SASP, termed $\alpha^-\beta^-$ spores, are more sensitive to wet heat, which kills $\alpha^-\beta^-$ spores by DNA damage including depurination. Some peroxides (e.g., H_2O_2), also kill $\alpha^-\beta^-$ spores by DNA damage, although they probably kill wild-type spores by damage to some core protein(s).

While some toxic chemicals kill spores either by DNA damage or damage to some spore core protein(s), many toxic chemicals used in the killing of spores, including chlorine dioxide (ClO_2), hypochlorite (OCl^-), and iodine, kill spores by damaging the spores' IM, such that the IM ruptures when the treated spores germinate (Cortezzo et al., 2004; Setlow, 2006; Leggett et al., 2012). Treatment with these agent(s) also seems to somehow alter the IM in dormant spores, such that: *i*) the IM permeability increases dramatically; and *ii*) the IM is less able to withstand a thermal stress, and DPA is released at much lower temperatures than corresponding untreated spores. Further indications of damage to spores by a number of oxidizing agents are that: *i*) treated spores germinate quite slowly, even if some of the germinated spores do ultimately give rise to colonies upon plating; and *ii*) recovery of colonies from such treated spores is extremely sensitive to increased salt concentrations in the recovery media. However, the nature of the damage affecting the spores' IM leading to these effects is not known.

While the mechanisms of spore killing and of spore resistance are known for many of the agents used to kill spores in applied settings - wet heat, radiation, chemicals such as hypochlorite or chlorine dioxide - there is a lack of definitive studies on the exact mechanisms of spore killing by

and resistance to high hydrostatic pressure (HP) and various types of plasmas. In the case of HP, treatments at HP ≈ 400-700 MPa (levels proposed for food processing) do not efficiently kill spores, unless accompanied by elevated temperature (T = 90 – 121 °C). Spore killing by HP treatments takes place in (at least) two steps; first, spores are germinated by the HP, then the much less resistant germinated spores are killed at the elevated temperatures at which HP treatments are carried out.

Generally, moderate HPs (100-350 MPa, T = 37 °C) trigger germination by activating the same GRs that trigger spore germination with nutrients, while HPs of 400-900 MPa (T ≥ 50 °C) appear to directly open the channel through which CaDPA is normally released during germination (Setlow, 2007; Reineke et al., 2013a; Reineke et al., 2013b). Recent studies have indicated that HP treatments in the regime P = 550-692 MPa and T = 75-112 °C induce spore activation (potentiate spores for germination), and this can even increase apparent spore titers (Luu et al., 2015). This latter effect has been seen with spores of the model spore former, *B. subtilis*, and also with spores of *Bacillus amyloliquefaciens*, a suggested surrogate for *Clostridium botulinum* spores in HP studies (Margosch et al., 2004; Sevenich et al., 2014). Other recent work (Kong et al., 2014) with *B. subtilis* spores has shown that: *i*) 140 MPa HP treatments as short as 10 sec can commit spores to germinate for up to 10 min during holding at atmospheric pressure; and *ii*) almost all spores go on to germinate over > 45 min after a 10 sec 140 MPa HP treatment during holding at 1 MPa, a pressure that alone does not induce germination. These latter findings indicate that at least some of the effects of 140 MPa of HP that can lead to spore germination are reversible, and thus the reversible events take place before events that irreversibly commit spores

to germinate. It will be of interest to examine these same phenomena in spores exposed to HPs ≥ 500 MPa (the HP that opens channels for CaDPA release in *B. subtilis* spores).

In the case of cold plasma, when significant levels of UV photons are associated with a particular type of plasma, there is evidence that these plasmas kill spores by DNA damage and α/β-type SASP and DNA repair are important in spore resistance to such plasmas (Roth et al., 2010; Yardimci and Setlow, 2010; Klämpfl et al., 2012; van Bokhorst-van de Veen et al., 2015). For plasmas that have minimal associated UV photons, mechanisms of spore killing and resistance are less clear. There is certainly evidence that plasmas with oxygen in the feed gas can cause significant physical damage to spores by etching the spores' outer layers. However, it is likely that this physical damage is not what actually kills spores, and research is needed to establish definitively mechanisms of spore killing by and resistance to various plasmas, including those that contain minimal levels of UV photons.

3.0 AFM Characterization of Morphological and Structural Attributes of *Bacillus* Spores

Atomic Force Microscopy (AFM) can be used to analyze high-resolution architecture, assembly, structural dynamics, and function of dormant and germinating spores of various wild type and mutant *Bacillus* species (Plomp et al., 2005a,b,c; Plomp et al., 2007a; Carroll et al., 2008; Ghosh et al., 2008; Plomp and Malkin, 2009; Malkin and Plomp, 2010; Malkin, 2011; Plomp et al., 2014; Ejhadj et al., 2015) and *Clostridium* (Plomp et al., 2007b). Specifically, AFM has been used to directly visualize and analyze spore morphological, dimensional, and high-resolution coat structural attributes, and these results demonstrated that spore morphological and coat

structures are phylogenetically (Plomp et al, 2005abc; Plomp et al., 2014) and growth medium (Malkin, 2011; Elhadj et al., 2015) dependent. We have found that strikingly different species-dependent spore coat structures are a consequence of nucleation and crystallization mechanisms that regulate the assembly of the outer spore coat (Plomp et al., 2005a,b,c; Plomp et al., 2007b; Malkin and Plomp, 2010). Spore morphological, dimensional, and structural attributes could serve as a baseline for assessing the effects of sterilization and/or decontamination treatments on the morphological and structural integrity and the ultra-structural damage of spores treated by irradiation or ClO_2.

3.1 Materials and methods

Detailed experimental procedures for AFM imaging of spores were described previously (Plomp et al., 2005a,b; Plomp et al., 2014). Droplets (~2.0 μl) of spore suspensions were deposited on plastic cover slips and incubated for 10 min at room temperature, then the sample substrate was carefully rinsed with double-distilled water and allowed to dry. Images were collected using a Nanoscope IV Atomic Force Microscope (Bruker Corporation, Santa Barbara, CA) operated in tapping mode. For rapid, low-resolution analysis of spore samples, fast scanning AFM probes (DMASP Micro-Actuated, Bruker Corporation, Santa Barbara, CA) with resonance frequencies of ~210 kHz were utilized. For high-resolution imaging, SuperSharpSilicon (SSS) AFM probes (NanoWorld Inc, Neuchâtel, Switzerland) with tip radii < 2 nm and resonance frequencies of ~300 kHz were used. Nanoscope software 5.30r3sr3 was used for data acquisition and subsequent processing of AFM images. In order to assess low-resolution and high-resolution spore features, raw AFM images typically needed to be modified. In particular, the *contrast enhancement* command, which runs a statistical differencing filter on the acquired image, was

typically utilized to bring all of the features of an image to the same height and to equalize the contrast among them. This allows all features of an image to be seen simultaneously, and thus a single spore or a group of spores can be imaged at relatively low resolution while spore coat attributes can be visualized at high resolution. Heights of spore surface features (i.e. folds, coat layers, etc.) were measured from *height* images using the *section* command. Tapping amplitude, phase, and height images were collected simultaneously. Height images allow quantitative height determinations, providing precise measurements of spore surface topography. Amplitude and phase images do not provide height information, but provide similar morphological and structural information as height images, often displaying a greater amount of structural detail and contrast compared to height images and making them a preferred choice for presentation purposes. Prior to AFM characterization, spore preparations were examined for refractility by phase-contrast light microscopy (Nikon Eclipse 50i).

3.2 AFM Characterization of gamma-irradiated *Bacillus* spores.

3.2.1. Native air-dried Bacillus spore. Size distributions (spore height/width and length) from large populations (several hundreds) of air-dried solution- and agar-grown spores were determined for spores of *B. atrophaeus, B. thuringiensis, B. subtilis* (Plomp et al., 2005a) and *B. anthracis* spores (Elhadj et al., 2015), with more than 30 spore preparations being utilized for the assessment of *B. anthracis* spore dimensional attributes (Elhadj et al., 2015). Representative results are compiled in Table 4.

Typical AFM images of *B. anthracis* and *B. thuringiensis* spores are presented in Figures 5a and 1b, respectively. The corresponding optical phase microscopy is shown in (Figures 5c,d), demonstrating that these spores are phase bright (refractile, ungerminated). The vast majority of spores (Figure 5a,b) are intact with heights within ranges indicated in Table 4 above and exhibiting surface ridges (some indicated with white arrows) extending along the long axis of the spore. These ridges are the characteristic attribute of air-dried *Bacillus* spores (Plomp et al., 2005abc; Plomp et al., 2014) and appear due to coat folding caused by changes in spore size upon dehydration (Driks, 2003; Westphal et al., 2003; Plomp et al., 2005a). Occasionally, collapsed spores (as one indicated with a black arrow in Fig. 5a) with heights in the range of 200 – 500 nm are observed in the spore preparations. This phenomenon could be attributable to partial germination, and subsequent partial collapse of the germinated spore upon air drying due to germination-induced internal structural changes.

3.2.2. Gamma-irradiated Bacillus spores. Dauphin et al. (2008) reported that subjecting virulent *B. anthracis* spores at a concentration of 10^7 CFU/ml to a dose of 2.5×10^6 rads results in complete spore inactivation (sterilization). The spore images shown below in Figures 6-9 were certified as sterilized for shipping and likely to have received a standard dose higher than 2.5×10^6 rads to assure sterility. Specifically, we characterized gamma-irradiated *B. anthracis* Ames spore samples produced on Nutrient sporulation medium (NSM) agar, Nutrient agar-BBL, Mueller Hinton-BBL, and Brain Heart Infusion (BHI)-BBL using AFM imaging and demonstrated that upon dehydration, as illustrated in Figure 6, the architecture of these spores collapsed. AFM examination of irradiated spores prepared as air-dried samples revealed further pronounced morphological and structural differences from native spores (Figure 5 a,b). As

illustrated in Figure 7, air-dried samples of gamma-irradiated spores comprised partially collapsed spores (PCS), spore coat remnants (SCR), and exosporia remnants (ER). The heights of PCS were in the range of 400-600 nm, which is significantly lower than the height of an air-dried non-irradiated native spores (Table 4). The thickness of SCR and ER was in the range of 100-250 nm and 40-45 nm respectively, which are comparable with the dimensions of native spore coats and exosporia. Only a small proportion of the air-dried samples of gamma-irradiated *B. anthracis* Ames spores were present as intact spores (IS, Figure 7d) exhibiting heights equal to non-irradiated air-dried *B. anthracis* spores.

These studies demonstrated that exposure to sterilizing gamma-irradiation produced profound structural changes in *B. anthracis* spores. Irradiation damaged spore internal structural integrity (membranes, cortex etc.) and caused either partial (PCS) or complete (SCR) evacuation of the spore core. It is likely that in the hydrated sample, internal spore components (protein, DNA, ribosomes, small molecules, etc.) have partially/or completely diffused from the spore core into the bulk liquid phase. Note, that the leakage of spore core contents into the bulk media could also adversely affect biochemical and chemical analysis of the collected irradiated sample. Because of the significant internal structural damage induced by irradiation, the dehydration of irradiated spores suspended in liquid resulted in their collapse (Figures 6,7).

There was an excellent cross-correlation between phase contrast optical microscopy and AFM in the characterization of the irradiated spore samples. Thus, as seen in Figure 8, phase contrast microscopy demonstrated that the vast majority of spores in irradiated samples were either phase

dark, which corresponds to the evacuation of the spore coat, or spore ghosts, which corresponds to spore coat remnants.

With AFM of air-dried spores for gamma-irradiated *B. thuringiensis* spores, similar types of ultrastructural damage and collapse have been observed (Figure 9). These samples comprise PCS with heights in the range of 30-40% of the height of non-irradiated native air-dried *B. thuringiensis* spores.

3.3. AFM Characterization of chlorine dioxide-treated *Bacillus* spores.

ClO_2 is sporicidal and a well-known decontamination regime for spores of *B. anthracis*. As illustrated in Figure 10, *B. atrophaeus* spores exposed to sporicidal levels of chlorine dioxide (dose = 2500 ppm-h) remain intact upon air-drying. The height of the chlorine dioxide-treated spores varies in the range of 500-650 nm, which corresponds well with the height of native air-dried *B. atrophaeus* spores (Plomp et al., 2005a). Similarly, the morphology of ClO_2-treated *B. atrophaeus* spores is indistinguishable from the morphology of untreated spores with pronounced surface ridges seen in Figure 5a. Furthermore, ClO_2 is a selective oxidant affecting cysteine, tryptophan and tyrosine amino acids in proteins and is not expected to grossly alter spore coat ultrastructure. Indeed, the high-resolution spore coat architecture and topology of ClO_2-treated spores is unaltered in character from those of native air-dried spores (Plomp et al., 2005a,b,c; Plomp et al., 2014), with rodlet coat structures and patches of an amorphous outermost layer clearly seen (Figure 10b).

3.4. AFM Characterization of Spore Responses in the Fully-hydrated vs. Air-dried State.

AFM allows a direct comparison of fully hydrated and air-dried native spores visualized under water and in air, respectively. Particularly, AFM studies of fully hydrated *B. atrophaeus* (Plomp et al., 2005a; Plomp et al., 2007a), *B. anthracis* (Plomp and Malkin, *unpublished results*) and *Clostridium novyi* NT spores (Plomp et al., 2007b) demonstrated that high-resolution attributes (i.e., rodlet, honeycomb, and inner coat layer structures), maintained the same patterns, lattice periodicities, and step heights as seen with air-dried spores (Plomp et al., 2005a,b,c; Plomp et al., 2014; Plomp et al., 2007b; Elhadj et al., *in preparation*). Furthermore, the ability of the coat to fold and unfold concomitant with changes in spore size was suggested (Driks, 2003; Westphal et al., 2003) based on measurements of *B. thuringiensis* spore dimensions induced by humidity transients. Images of a fully hydrated *B. atrophaeus* spores are presented in Figure 11a. Surface ridges, the prominent structural features of air-dried spores (Figure 5), are typically absent from the surface of fully hydrated spores (Figure 11a). The direct visualization of 35 individual spores was performed to probe the dynamic response of their aqueous to aerial phase transition (Plomp et al., 2005a) Spores were visualized under water, then air-dried for ~ 40 hours and imaged in air (65% relative humidity), then re-imaged after rehydration. Typical examples of hydration/dehydration ultrastructural transitions are presented in Fig. 11a,b. As illustrated in Figure 11a, the coat of a fully hydrated spore appears to be tightly attached to the cortex and upon dehydration (Fig. 11b) forms an ~50 nm surface ridge/fold extending along the entire length of the spore.

The changes in spore surface architecture with dehydration were accompanied by a decrease in spore size. As illustrated in Fig. 11c, the average width/height of 35 individual air-dried spores was reduced to 88% of the size measured for fully hydrated spores. The rehydration of air-dried

spores, by placing them in water for 2h, restored the spores to 97% of their original size, thereby establishing the reversibility of the size transition concurrent with rehydration (Fig. 11c).

The observed decrease in the width of bacterial spores with dehydration is apparently due to the contraction of the spore core and/or cortex. The spore coat itself does not shrink/expand but is flexible enough to compensate for the internal volume decrease of core/cortex compartments by surface folding and the formation of ridges. These studies establish that dormant spores are dynamic physical structures, which exhibit profound morphological and structural responses with changes in its natural environment. These changes play important roles in selecting and implementing successful decontamination strategies.

4.0. Bio-indicators for the Inactivation of *Bacillus spp.* Spores by ClO_2 Gas

As a gas-phase sporicide, ClO_2 has advantages over other gas-phase sterilizing agents that leave residues or may pose health hazards (Bruch, 1973; Dolovich et al., 1984; Chapman et al., 1986; Lettman et al., 1986; Lykins et al., 1994; Muttamara et al., 1995). The efficacy of ClO_2 decontamination treatments are typically verified through the use of spore Biological Indicators (BIs). We present extensive statistical analysis and modeling results that can be used to predict survival probabilities for three species of spores at varying doses of ClO_2 by analyzing its effectiveness to kill 6 logs of bacterial spores (sterilize). Our analysis includes four lots of *B. atrophaeus* spore strips with different D values for ethylene oxide (D_{EtO}) to allow their use as BI's to monitor process efficacy in large-scale emergency decontamination efforts, as well as the spores of *G. stearothermophilus* and *B. thuringiensis*, a close relative of *B. anthracis*. Parameters

contributing to the efficacy of spore sterilization by ClO_2 include, but are not limited to, ClO_2 concentration, relative humidity (RH), temperature, exposure time, and the BI packaging materials.

4.1. Materials and methods

4.1.1. Spore strips. Spore strips (Raven Biological Labs, Omaha, NE) are inch-long pieces of cellulose paper inoculated with a known concentration of bacterial spores, and packaged in a barrier material that permits the diffusion of a sterilant gas (e.g. ethylene oxide, abbreviated EtO, steam, or ClO_2) or humidified air, but excludes contaminants such as vegetative bacterial cells or other spores. Spore strips act as BI's for various processes (EtO, autoclaving, irradiation, ClO_2) to achieve sterilization. Three *Bacillus* spore species were assayed for susceptibility to ClO_2: *B. atrophaeus* (ATCC 9372, formerly *B. subtilis* var. niger and *B. globigii*), *B. thuringiensis* (ATCC 29730), and *Geobacillus stearothermophilus* (ATCC 7953, formerly *Bacillus stearothermophilus*). Spore strip populations for all species were determined by the manufacturer, as were D and Z values for two of the three species. D values for ethylene oxide (D_{EtO}) and dry heat (D_{160}) were determined for *B. atrophaeus*, while D values for saturated steam (D_{121} and $D_{132.2}$) were determined for *G. stearothermophilus*. No such values were determined for *B. thuringiensis*. Species lot numbers, populations, and relevant D and Z values are listed in Table 5.

4.1.2. BI packaging material. BI packaging is a crucial factor in the efficacy of the ClO_2 sterilizing process. In this report, we primarily investigate the sporicidal bioeffects of ClO_2 on BI's packaged either in 1059B medical grade Tyvek (single-sided with a plastic backing)

(Raven) or nothing, as our preliminary data suggested that 1059B was relatively non-reactive and non-attenuating for ClO_2. To comply with current industry standards, we also show that ClO_2 is an efficacious sterilant of *B. atrophaeus* BI's packaged in medical grade glassine (Raven).

4.1.3. ClO_2 generation and treatment. ClO_2 was generated by the oxidation of technical grade sodium chlorite ($NaClO_2$) by sodium persulfate ($Na_2S_2O_8$) (Sigma) in aqueous solution:

$$2\ NaClO_2 + Na_2S_2O_8 \rightarrow 2\ ClO_2 + 2\ Na_2SO_4$$

Pure gaseous ClO_2, free of volatile by-products such as Cl_2, was purged from the reaction flask and diluted with ratios of filtered, dehumidified and humidified air to attain the target $ClO_{2(g)}$ concentration and RH conditions. RH was controlled with a series of flow meters (Cole Parmer) passing filtered and dehumidified air through a 500 ml gas wash bottle half filled with deionized water. The humidified diluted gas was directed into a 5 L glass test chamber (Fisher), and ClO_2 concentration ($[ClO_2]$) in parts per million (ppm) was determined by iodometric titration of a 50 or 100 ml volume/sample of gas taken/removed/sampled from the exit port of the reaction chamber in a gas-tight Hamilton sample-lock syringe (Fisher). Experiments were carried out at ambient temperature and atmospheric pressure (measured and monitored with a Traceable® Digital Hygrometer/Thermometer, VWR), with RH ranging from 30-90%, and $[ClO_2]$ ranging from approximately 50-2000 ppm. Experimentally measured values for temperature, RH and $[ClO_2]$ are listed in Table 6.

In order to guarantee contact with ClO_2, no more than 20 spore strips were placed in the test chamber at one time, and, thus, multiple runs at each reported dose were performed in order to *i*) assure repeatability of our results, and *ii*) gather enough data to achieve statistically significant results (Table 7). One negative control strip (no inoculum and packaged appropriately) was included in the chamber for each set of 10 test strips, and a positive control strip remained outside of the test chamber and away from other potential sterilizing agents for the duration of each experiment.

4.1.4. Microbiological assays of sterility. After exposure to the appropriate ClO_2 dose, the strips were placed, using aseptic technique, into tubes of Tryptic Soy Broth containing a Bromocresol Purple pH indicator (Raven) and incubated at 37 ^{o}C (*B. atrophaeus* and *B. thuringiensis*) or 60^{o}C (*G. stearothermophilus*) for 7 days. We monitored the tubes on a daily basis for both turbidity (indicative of bacterial growth) and color change of the pH indicator from purple to yellow (indicative of metabolism). Criteria for a strip being considered "killed" were findings of both *no* turbidity and of *no* color change of the pH indicator, coupled with growth and metabolism for the positive control associated with the sample test set and no growth for the negative control.

4.2. Statistical Analysis and Modeling

We fitted a binomial generalized linear model with a complementary log-log link function to the proportion of strips still having live spores after treatment, allowing the dispersion parameter to be greater than one to account for over-dispersion. We adjusted for covariates such as (logarithm of) the number of spores on a strip, the type of packaging used to store the spore strips, RH, and D_{EtO} values. The model in its most general form is expressed as equation (1)

$$\log(-\log(1-Ø)) = b_0 + b_1*Dose + b_2*\log N + b_3*Pack + b_4*RH + b_5*D_{EtO} \quad (1)$$

in which Ø is the probability of a strip still having living spores after treatment, p_N is the probability of a spore remaining alive after treatment (depends on N), *Dose* is the dose of ClO_2 as calculated by ClO_2 ppm multiplied by exposure time (in units of hours), N is the number of spores on a strip, *Pack* equals 1, if spore strips came in Tyvek packaging, and *Pack* equals 0, if there were no packaging, *RH* is the relative humidity (as a proportion), D_{EtO} is the time (in units of minutes) to reduce the number of living spores to 10% of the original value by ethylene oxide (Table 5), and b's are regression coefficients. The relationship between the strip survival probability Ø and the spore survival probability p_N is expressed in equation (2)

$$1 - Ø = (1 - p_N)^N \quad (2)$$

and equation (1) can be re-written as equation (3)

$$\log(-\log(1-p_N)) = b_0 + b_1*Dose + (b_2 - 1)*\log N + b_3*Pack + b_4*RH + b_5*D_{EtO} \quad (3)$$

The range of values of each of the covariates in the various experiments is described in (Table 7). Although the independent variable is the strip survival probability Ø, Figure 12, Figure 13, and Figure 14 are reported in terms of our primary measure of interest, which is the probability p_N that any single spore survives.

The data in Figures 12A,B,C,D clearly demonstrate that the probability, with a confidence level of 95%, of a spore surviving greatly diminishes as dose increases. In fact, the correlation between increasing [ClO_2] and sporicidal activity is strong for all species and lots tested. At a constant spore strip population (1.2×10^6), exposure time, and %RH (79%), the percent of spore strips killed increases (probability of a spore surviving decreases) as a function of increasing dose (does ≡ ppm ClO_2 × exposure time) as the gas concentration increases (Figure12A,B Similarly, we have also found that for a constant [ClO_2], RH, and spore population, increasing the dose by increasing the exposure time also results in higher levels of kill (lower probability of survival, Figure12C,CD).

A particular point of interest is the dose at which the predicted spore survival probability is at most 10^{-6} (the EPA target) with 95% confidence. If we consider species *B. atrophaeus* as an example, for which there is a D_{EtO} value of 3.1 or 5.0, an RH of 0.79, and take the number of spores to be 10^6 (not stratifying by packaging), then the dose at which a 6-log drop is achieved is, with 95% probability, between 268 − 592 or between 628 − 822 ppm-hours, respectively (data not shown), which is significantly less than the dose of 2500 ppm-hours required in some whole building decontaminations. This suggests that a lower D_{EtO} value correlates with a greater susceptibility to ClO_2, a phenomenon that we also see graphically in Figures 13A,B,C,D). Though *B. atrophaeus* spores are accepted as a standard test organism for sterility (Rosenblatt et al., 1987), the strains of *G. stearothermophilus* and *B. thuringiensis* spores assayed required higher ClO_2 doses (at 0.79 RH), between 1235 − 2415 ppm-hours and 1497 − 2063 ppm-hours, respectively, to achieve the same spore survival probability ($\leq 10^{-6}$) with 95% confidence (Figures 12A,B).

With [ClO_2] = 500 or 1000 ppm and exposure time fixed at 4 h, we varied the %RH (40%-90%) of the exposure chamber to assess the bioeffects of humidified ClO_2 on two lots of *B. atrophaeus* BI's with D_{EtO} values of 3.3 and 3.8 (Figures 13C,D). We found, in general, that increasing %RH at a given dose increases the level of kill (Figures 14A,B). Additionally, to achieve equivalent levels of kill at a fixed ClO_2 dose, higher RH is required for *B. atrophaeus* strips with a higher D_{EtO} value (Figure 14A,B). In general, we found that RH levels of $\geq$80% are optimal for ClO_2 sporicidal bioeffects over a wide range of doses.

The humidity dependence of ClO_2 sterilization may be two-fold. Increasing RH results in an increase in localized sorption of water molecules on the spore surface, causing the spore to swell and hypothetically resulting in increased pore size through which ClO_2 can pass (Westphal et al., 2003). ClO_2 partitioning from the gas phase into aqueous solution is about 1:40, and it has been reported that ClO_2, a radical, is a dissolved gas in solution (Simpson et al., 1993; Aieta and Berg, 1986). Therefore, as RH increases, thus does the local concentration of ClO_2, and the spore becomes more swollen, perhaps more readily passing water and its associated dissolved ClO_2 gas through opened channels. Other authors have reported a similar relationship between increased RH during ClO_2 treatment with increased mortality of vegetative bacterial cells (Han et al., 1999; Han et al., 2001).

We consistently observed no statistically significant difference in spore killing between BI's packaged in 1059B medical grade Tyvek versus no packaging (Figure 12, Figure 13, and Figure 14). Identical lots of *B. atrophaeus* log 6 spore strips, 1161841 and 1161911, with D_{EtO} values of

3.3 and 3.8, respectively, and packaged by the manufacturer in their standard and industry-accepted medical grade glassine, yielded grossly inconsistent results when exposed to a wide range of ClO_2 doses (data not shown) – at 2000 ppm-hours and 80% RH, 90% of the spore strips (lot 1161841) were killed when packaged in Tyvek and there was no effect on the strips packaged in glassine (Figure 14C). A much greater dose (~20,000 ppm-hours) was required to kill 100% of the *B. atrophaeus* strips packaged in glassine (Figure 14D). Figure 14E shows predicted probabilities of a spore remaining live after treatment, for Tyvek and no packaging, for all three species (two different D_{EtO} values for *B. atrophaeus*) and with RH = 0.79 and the number of spores fixed at $N = 10^6$.

5.0 Conclusions

Moving exciting research findings from the benchtop to the hands of the end-user as novel technologies is a paramount goal of Science and Technology (S&T) for many government research and development (R&D) facilities. The novel ClO_2 decontamination technologies invented at NSRDEC serve as a model for successful federal research and development work, Technology Transfer, commercialization, and deployment for actual use in the field. In fact, this work began with basic research in the mechanisms of bacterial spore inactivation, then transitioned to early exploratory research and development work focused on the chemical reaction kinetics and mechanisms of ClO_2 formation occurring through a unique chemical effector. Later development work consisted of inventions, validating efficacy, obtaining patents, and eventually transitioning to private industry through Technology Transfer for

commercialization in the marketplace. This technology has become a COTS item that enables its recent culmination as Field Decontamination Kits (FDKs) deployed at clinical sites in West Africa for the sterilization of Ebola-contaminated medical devices at a time when concern of the Ebola crisis in those regions and the fears of the virus spreading internationally were at their highest.

Scientists at NIH/NIAID (National Institutes of Health/National Institute of Allergy and Infectious Diseases) and USAMRIID (The U. S. Army Medical Research Institute of Infectious Diseases) adapted the COTS version of NSRDECs novel decontamination technologies and developed compact, lightweight, easy-to-carry Field Decontamination Kits (FDKs) for use by global public health organizations such as Doctors without Borders (MSF), the World Health Organization (WHO), Public Health Canada, National Institutes of Health (NIH), and the U.S. government to improve hygienic conditions in remote clinics where little infrastructure existed by sterilizing medical equipment and help fight the spread of a deadly disease that cost thousands of lives and untold costs in medical expenses caring for the afflicted.

NSRDECs novel decontamination technologies were readily available to help others meet and overcome the challenges and concerns of this international public health through R&D that strives for such preparedness. These novel technologies decontaminate microbes in myriad applications, such as rinses, sprays, and gas for fresh produce; food contact and handling surfaces; personal protective equipment; textiles used in clothing, uniforms, tents, and shelters; graywater; airplanes; surgical instruments; and hard surfaces in latrines, laundries, and deployable medical facilities.

One strength of NSRDECs novel decontamination technologies is that the mechanisms of bacterial spore inactivation by ClO_2 and the use of spore bio-indicators for ClO_2 in decontamination procedures have been investigated thoroughly at University of Connecticut Health Center, Lawrence Livermore National Laboratories, Children's Hospital of Oakland Research Institute, Stonehill College, and Brandeis University, making the fundamental science of ClO_2 generation and decontamination well-understood, and NSRDECs technologies more assured and reliable. We have also reviewed mechanisms of bacterial spore inactivation by novel, emerging, and established nonthermal technologies for food preservation, such as high pressure processing, irradiation, cold plasma, and chemical sanitizers, using an array of *Bacillus subtilis* mutants to probe mechanisms of spore germination and inactivation, demonstrating that understanding the basic science allows the development of innovative technologies that can find solutions in diverse applications outside of the pasteurization and sterilization of foodstuffs.

Acknowledgements.

Work carried out in the Setlow laboratory on spore resistance and killing has received generous support over many years from the Army Research Office, the Defense Threat Reduction Agency, and the National Institutes of Health.

The AFM work in the Malkin laboratory was performed under the auspices of the U.S. Department of Energy by Lawrence Livermore National Laboratory under Contract DE-AC52-07NA27344 and supported by a grant from the Federal Bureau of Investigation and by Lawrence

Livermore National Laboratory through Laboratory Directed Research and Development Grant 04-ERD-002. The authors are grateful to Marco Plomp for his critical contributions into the AFM characterization and data analysis.

The work in the Leighton laboratory was funded by The Defense Advanced Research Projects Agency (DARPA). We acknowledge with pleasure and gratitude the contributions of Katie Wheeler and Gordon Eggum to the study of ClO_2 bio-indicators.

We express our gratitude and appreciation to the US Army NSRDEC to support u sin undertaking this mission-critical R&D and to collaborate with experts from academia and other government agencies to complete this manuscript. We thank Mr. James M. Doona for helpful discussions of mathematics and Mr. Murphy C. Doona for assistance counting spores.

Tables

Table 1. Acronyms and attributes of NSRDEC decontamination technologies.

NCC	**N**ovel **C**hemical **C**ombination	Dry powders mix with water
PCS	**P**ortable **C**hemical **S**terilizer	Plastic suitcase sterilizer
D-FENS	**D**isinfectant-sprayer **F**or **EN**vironmentally-friendly **S**anitation	Collapsible handheld sprayer
D-FEND ALL	**D**isinfectant **F**or **EN**vironmentally-friendly **D**econtamination, **ALL**-purpose	All purpose decontamination
CoD	**C**ompartment **o**f **D**efense	In-package disinfectant
FDK	**F**ield **D**econtamination **K**it	Ebola disinfectant

Table 2. Laboratory tests of FDKs and the PCS.

Test code	Container	Conditions	Observations	Microbiological Results
Test a	2.5-gal bag	- 15g Part A - 4g Part B - 30 mL H_2O (tap) in 100 mL beaker	Reaction in 2:20 RH > 96.4% T = 30 °C [ClO_2] >7000 ppm	Sterilized[a,b]
Test h	10-gal bag	- 15g Part A - 4g Part B - 30 mL H_2O in 100 mL beaker	Reaction at 2:10 RH > 74% T = 25.4 °C	Sterilized[a,b]
Test i	PCS	- 16g Part A - 4g Part B - 30 mL H_2O in 100 mL beaker	Reaction at 2:30 RH > 90.2% T = 24.4 °C [ClO_2] >7000 ppm	Sterilized[a,b]
Test n	PCS	- 15g Part A - 4g Part B - 30 mL tap H_2O in 100 mL beaker	Reaction at 2:12 RH > 93.5% [ClO_2] >7000 ppm Run time 15 min	Sterilized[a,b]

[a,b] **sterility confirmed with *G. stearothermophilus* and *B. atrophaeus* bio-indicators.**

Table 3. Mechanisms of spore killing by and resistance to various agents*

Type of agent	Mechanisms of killing	Mechanisms of resistance
HP	Probably protein damage	low core water content
UV, γ-radiation, nitrite, formaldehyde	DNA damage	α/β-type SASP, DNA repair, and perhaps IM impermeability
Oxidizing agents (OCl^-, ClO_2, O_3)	IM damage	Spore coat/outer membrane
Hydrogen peroxide	Probably core protein damage	α/β-type SASP, low core water
OH^-, wet heat, some oxidizing agents	Inability to germinate	Spore coat/outer membrane
Strong mineral acid	Explosive rupture of IM	Not studied
Plasma	Protein or DNA damage[1]	α/β-type SASP, spore coat, DNA repair
Wet heat	Protein damage	α/β-type SASP, low core water content
Dry heat	DNA damage	α/β-type SASP, DPA, DNA repair

*Data for these conclusions are from Gerhardt and Marquis, 1989; Setlow, 1994; Setlow, 2001; Setlow, 2006; Setlow, 2007; Coleman et al., 2007; Coleman et al., 2010; Leggett et al., 2012; Setlow and Johnson, 2012; Reineke et al., 2013a; Reineke et al., 2013b; Moeller et al., 2014; Setlow et al., 2014.

[1]Plasma with UV-C kills spores by DNA damage, while UV-C free plasma likely kills by protein damage.

Table 4. Spore height determinations.

Spore species	Spore height Air-dried (solution-grown)	Spore height Air-dried (Agar-grown)
B. thuringiensis (1)	750 – 1000 nm avg ≈ 872 nm (AD = 5.4%)	740 – 1080 nm avg ≈ 937 nm (AD = 5.3%)
B. anthracis (11)	800 – 880 nm avg ≈ 835 nm (AD = 5.4%)	750 – 800 nm avg ≈ 780 nm (AD = 5.4%)

Table 5. Spore strip bio-indicator characteristics.

Species	ATCC #	Lot#	Population	D_{160} Value	D_{EtO} Value	Z-value
B. atrophaeus	9372	1162052	2.0 x 10^6	2.6	3.0	44.5
B. atrophaeus	9372	1161841	1.3 x 10^6	2.5	3.3	23.5
B. atrophaeus	9372	1161911	1.3 x 10^6	2.5	3.8	46.0
Batch 204GB:						
B. atrophaeus	9372	1142042	1.2 x 10^4	2.8	3.1	39.0
B. atrophaeus	9372	1152041	1.2 x 10^5	2.8	3.1	39.0
B. atrophaeus	9372	1162043	1.2 x 10^6	2.8	3.1	39.0
B. atrophaeus	9372	1172041	1.2 x 10^7	2.8	3.1	39.0
Batch 214GB:						
B. atrophaeus	9372	1142141	3.5 x 10^4	2.8	5.0	33.3
B. atrophaeus	9372	1152141	2.0 x 10^5	2.8	5.0	33.3
B. atrophaeus	9372	1162141	1.5 x 10^6	2.8	5.0	33.3
B. atrophaeus	9372	1172141	1.5 x 10^7	2.8	5.0	33.3
B. atrophaeus	9372	1182141	1.5 x 10^8	2.8	5.0	33.3
B. thuringiensis	29730	616022	1.2 x 10^6	n/a	n/a	n/a
				D_{121} Value	$D_{132.2}$ Value	Z-value
G. stearothermophilus	7953	3166031	1.0 x 10^6	2.0	0.07	7.5

Table 6. Experimental ClO_2 target and actual concentrations.

ClO_2 Concentration			ClO_2 Dose			Relative Humidity		
Target $[ClO_2]$ (ppm)	Measured $[ClO_2]$ (ppm)	Standard deviation	Target dose (ppm-hrs)	Measured dose (ppm-hrs)	Standard deviation	Target RH (%)	Measured RH (%)	Standard deviation
50	50	4	400 (Fig.1D)	414	20	30	30.32	0.0064
67	68	4	1000 (Figs.1C)	1037	32	40	38.75	0.0108
100	110	17	2000 (Fig.S1A)	2020	40	50	49.51	0.0145
125	131	6	4000 (Fig.S1B)	4046	88	60	59.41	0.0133
167	177	21				70	69.36	0.0107
200	218	14				80	79.42	0.0152
250	256	23				90	89.67	0.0074
400	405	31						
500	498	40						
800	784	53						
1000	1027	115						
2000	2027	303						

Room Temperature (degrees Celsius): 21.52, std. dev. 0.7703

Table 7. Tyvek spore strip data summary.

Species	Runs		*N*	Dose	RH	DEtO
	Tyvek	No package		(ppm ClO2 x time)		
B. atrophaeus	152	144	1.2 x 10^4 - 1.2 x 10^7	110 - 1991	79%	3.1
B. atrophaeus	490	350	3.5 x 10^4 - 1.5 x 10^8	110 - 1991	79%	5.0
B. atrophaeus	500	500	1.3 x 10^6	438 - 4106	30% - 90%	3.3
B. atrophaeus	498	495	1.3 x 10^6	438 - 4106	30% - 90%	3.8
B. thuringiensis	98	98	1.2 x 10^6	438 - 4106	79%	-
G. stearothermophilus	80	80	1.0 x 10^6	438 - 4106	79%	-

T = Tyvek, NP = no package

FIGURES

Figure 1. The PCS consists of a rigid plastic suitcase embellished with reactors, valves, scrubbers, and other design features to effectuate sterilization with ClO_2 while protecting users and the environment.

Figure 2. The D-FENS sprayer generates aqueous ClO_2 on-site and at point-of-use in a collapsible spray-bottle (left) and easily sprays ClO_2 onto contact surfaces (right) to wipe away contaminating pathogens in Army Field Kitchens and Navy galleys.

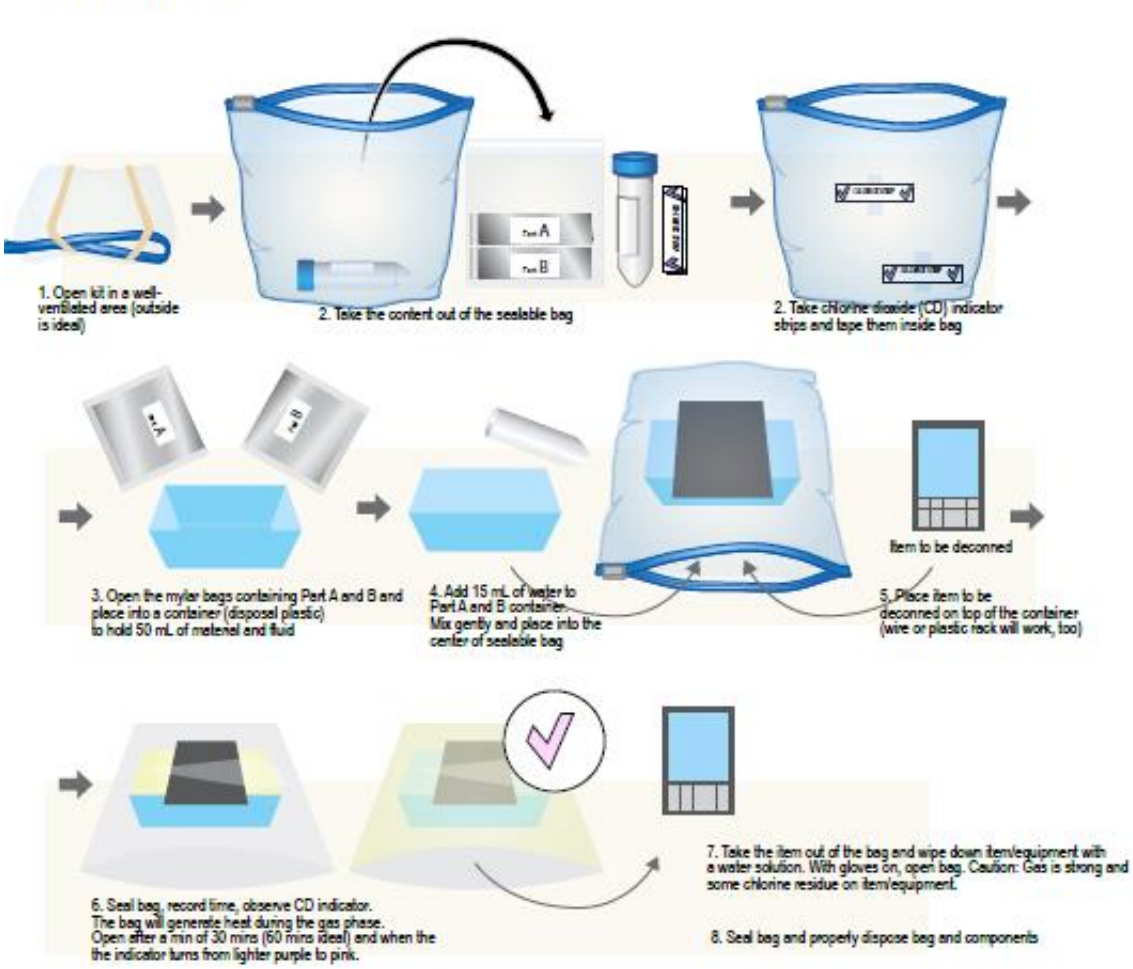

Figure 3. Diagrammatic of steps for using FDKs. Top Row. a) Open FDK in well-ventilated area (outdoors), b) remove contents form sealable bag, and c) tape ClO_2 indictor strips to inside of bag. **Middle Row.** a) Empty foil pouches of chemical reagents (Part A and Part B) into plastic container , b) add 15 mL of water with mixing, and c) place plastic container inside bag, then place contaminated medical device on top of container. **Bottom Row.** a) Seal bag, run for 30-60 min, and observe purple → pink color change of ClO_2 indicator strip, then b) with gloves on, open bag, remove device from bag, and re-seal bag for proper disposal. Caution: when opening bag, gas has a strong odor – avoid inhaling gas. With gloves on, use water to wipe residue from device/equipment.

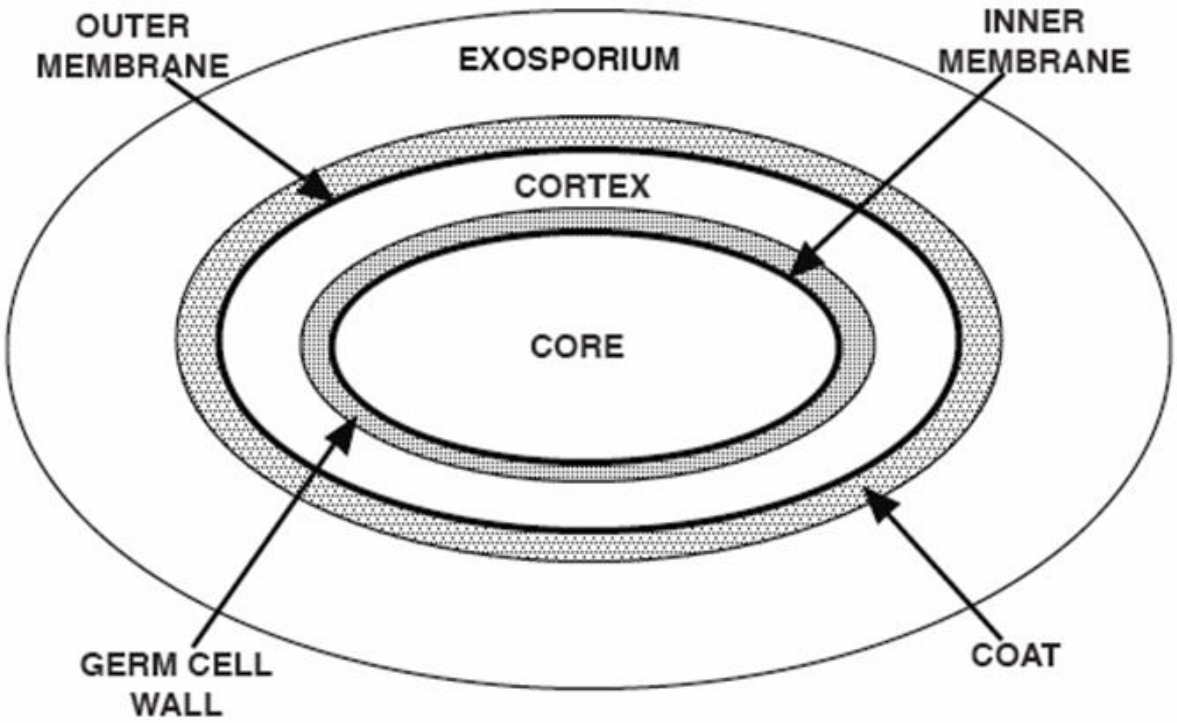

Figure 4. Spore structure. The various layers of a typical spore are shown in schematic form, and the various spore layers are not drawn to scale. Note that the exosporium is not present in spores of all species.

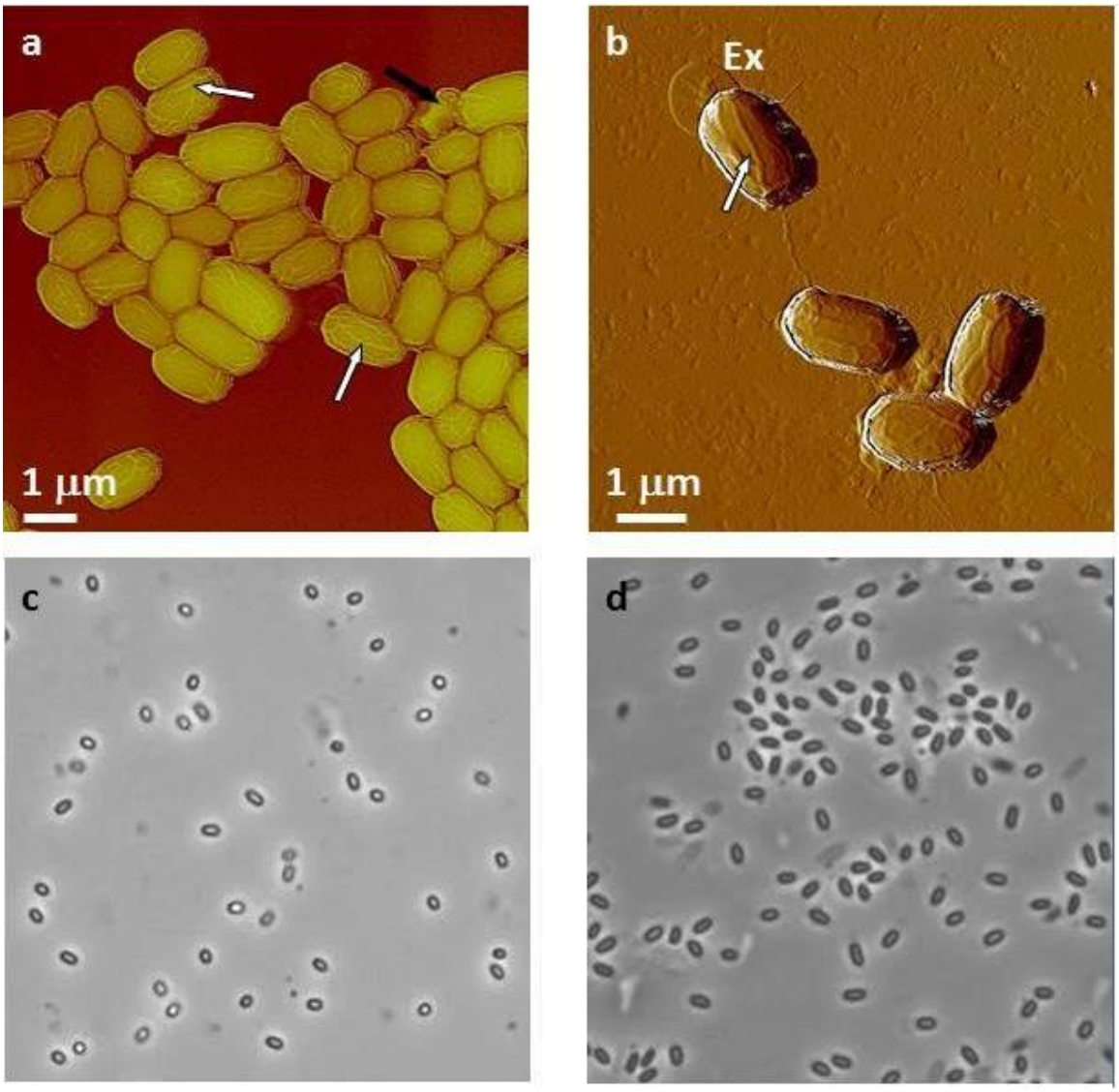

Figure 5. Characterization of *Bacillus* spores. (a,b) AFM images of native air-dried spores. (a) Height image of *B. anthracis* Sterne spores and (b) amplitude image of *B. thuringiensis* spores. In both images surface ridges extending along the entire length of spores (several surface ridges noted by white arrows) are seen. In (a) a collapsed spore is indicated with a black arrow. In (b) an exosporia is indicated with Ex. (c,d) Phase contrast microscopy images of *Bacillus anthracis* Ames spores (c) and *B. thuringiensis* spores (d).

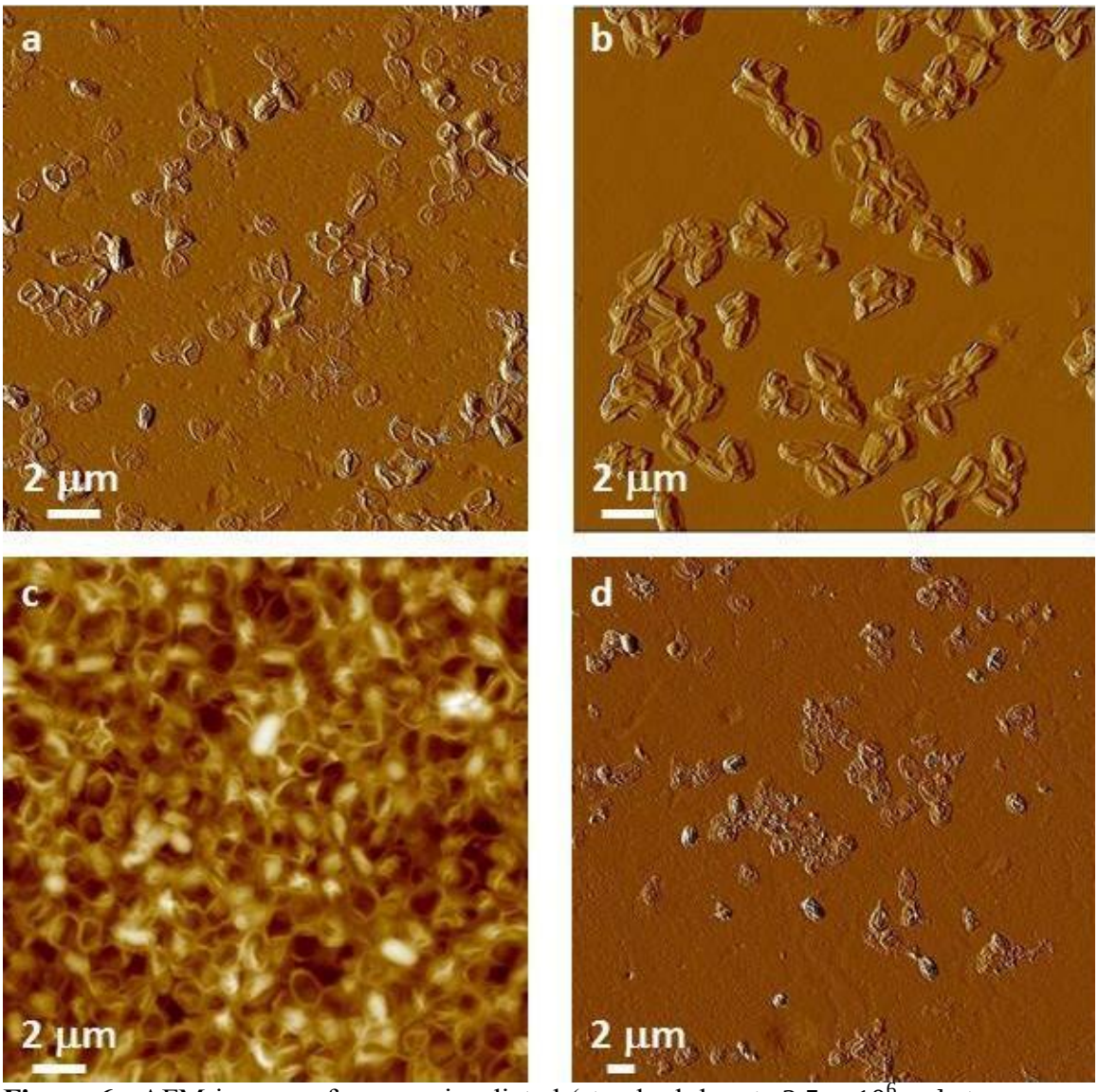

Figure 6. AFM images of gamma-irradiated (standard dose ≥ 2.5×10^6 rads to assure sterility) air-dried *B. anthracis* Ames spores**.** (a) spores produced on Mueller Hinton-BBL; (b) spores produced on NSM agar; (c) spores produced on nutrient agar-BBL; and (d) spores produced spores produced on BHI-BBL (a,b, d) and (c) are amplitude and height AFM images respectively.

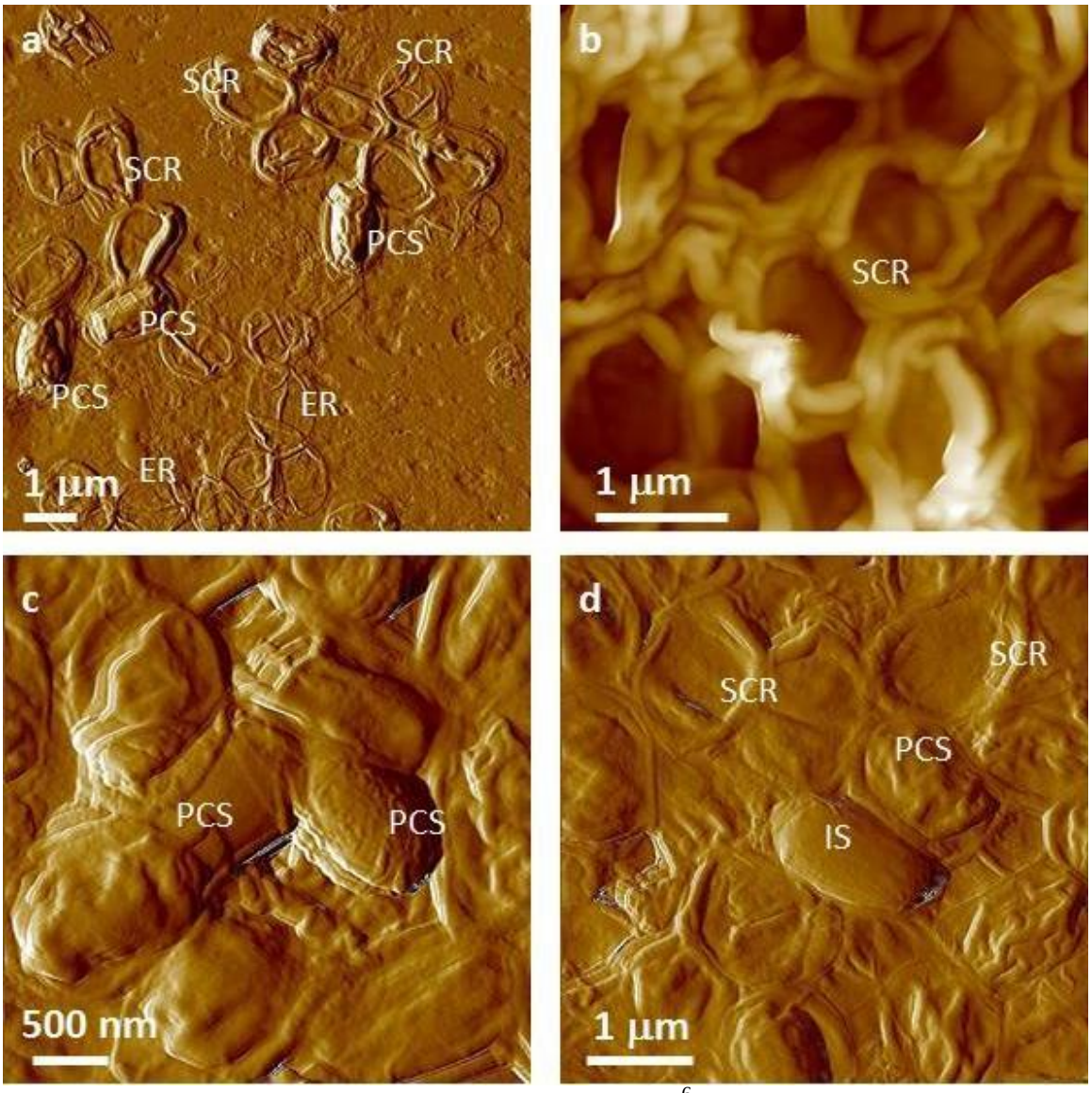

Figure 7. AFM examination of irradiated ($\geq 2.5 \times 10^6$ rads) *B. anthracis* Ames spore air-died samples. (a) spores produced on Mueller Hinton-BBL; (b) spores produced on NSM agar; (c,d) spores produced on nutrient agar-BBL. (a,c, d) and (b) are amplitude and height AFM images respectively.

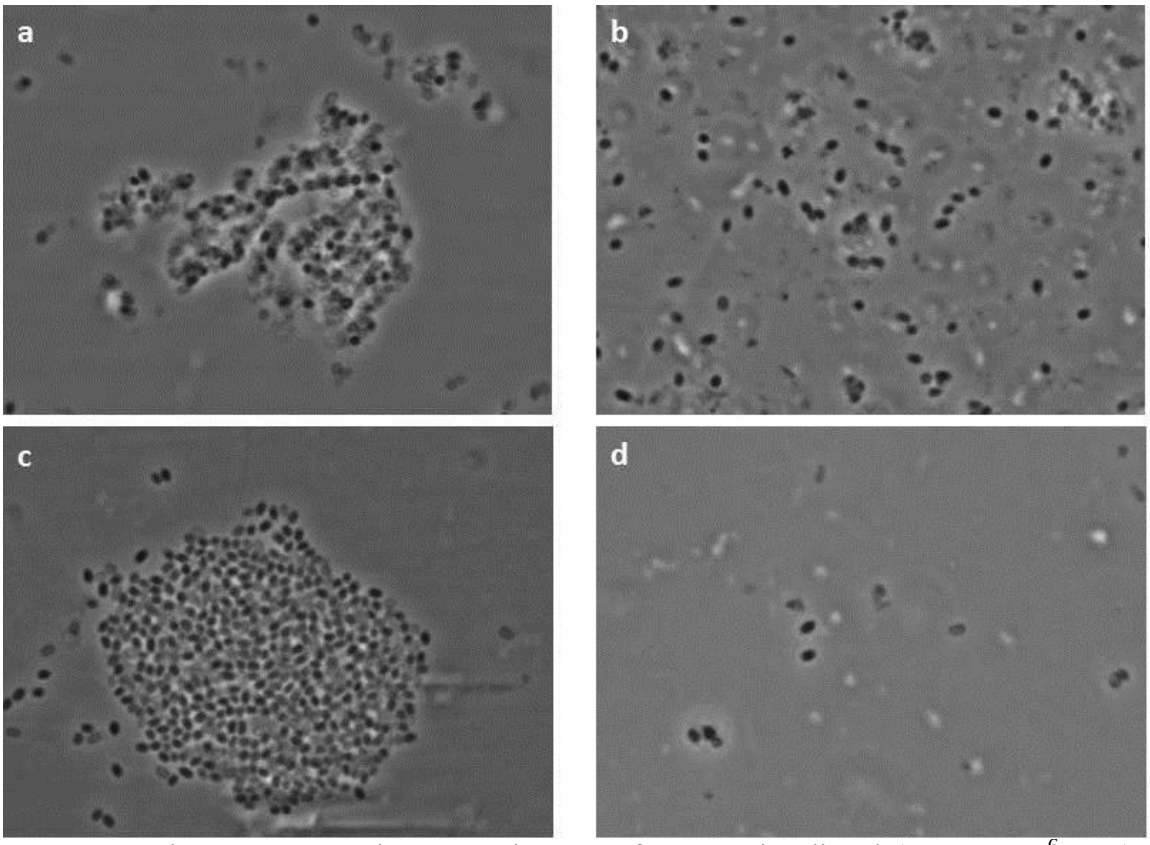

Figure. 8. Phase contrast microscopy images of gamma-irradiated (≥ 2.5 × 10^6 rads) *Bacillus anthracis* Ames spores grown on Mueller Hinton-BBL (a), NSM agar (b), nutrient agar-BBL (c), and BHI-BBL.

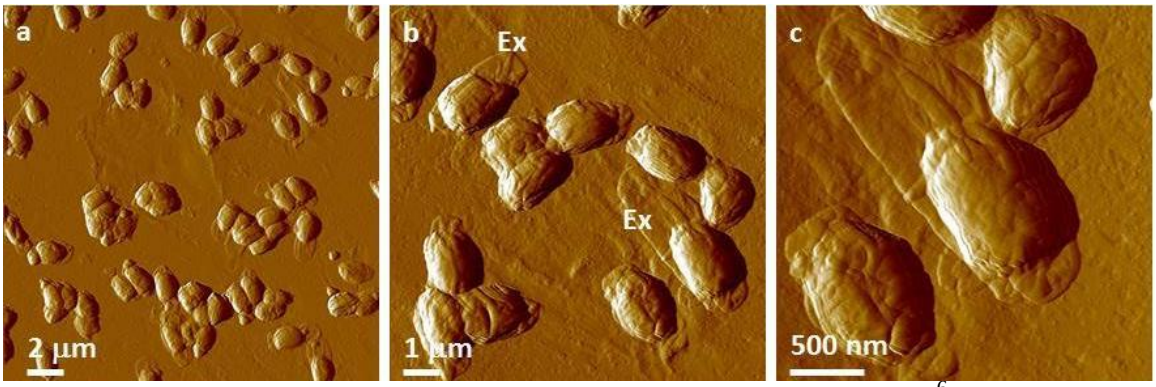

Figure 9. Amplitude AFM images of gamma-irradiated (≥ 2.5 × 10^6 rads) *B. thuringiensis* spores. In (b) an exosporia is marked with Ex.

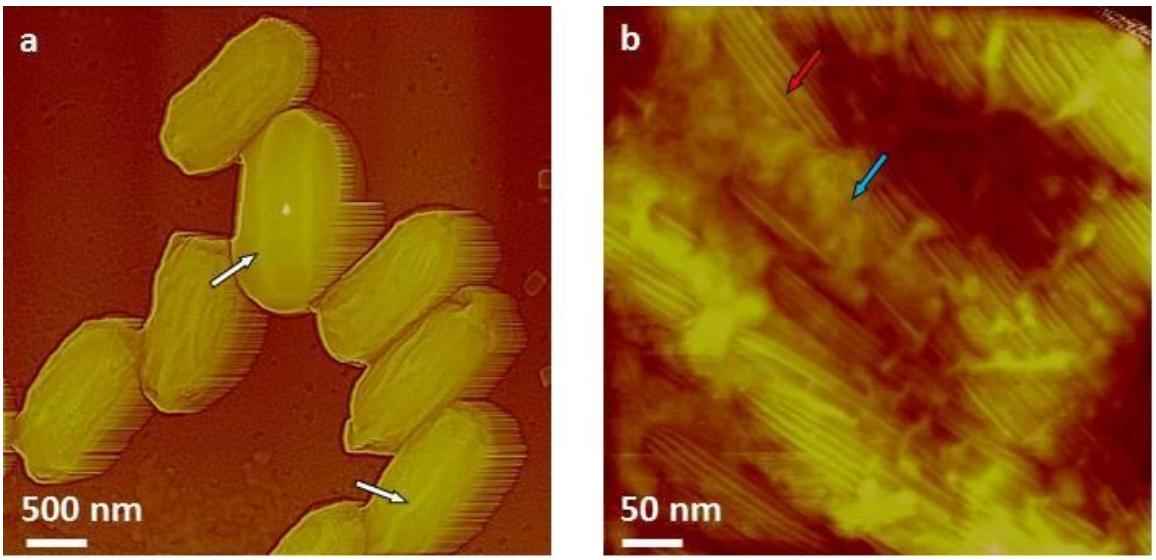

Figure 10. (a,b) Height AFM images of *B. atrophaeus* spores exposed to a sterilization (6-log kill) dose of ClO_2 (500 ppm × 5 h = 2500 ppm-h). In (a) surface ridges extending along the entire length of spores (several surface ridges noted by white arrows) are seen. In (b) High-resolution AFM image showing the regular rodlet structure (red arrow) and patches of an amorphous outermost layer (blue arrow), both characteristic to native, air dried *B. atrophaeus* spores.

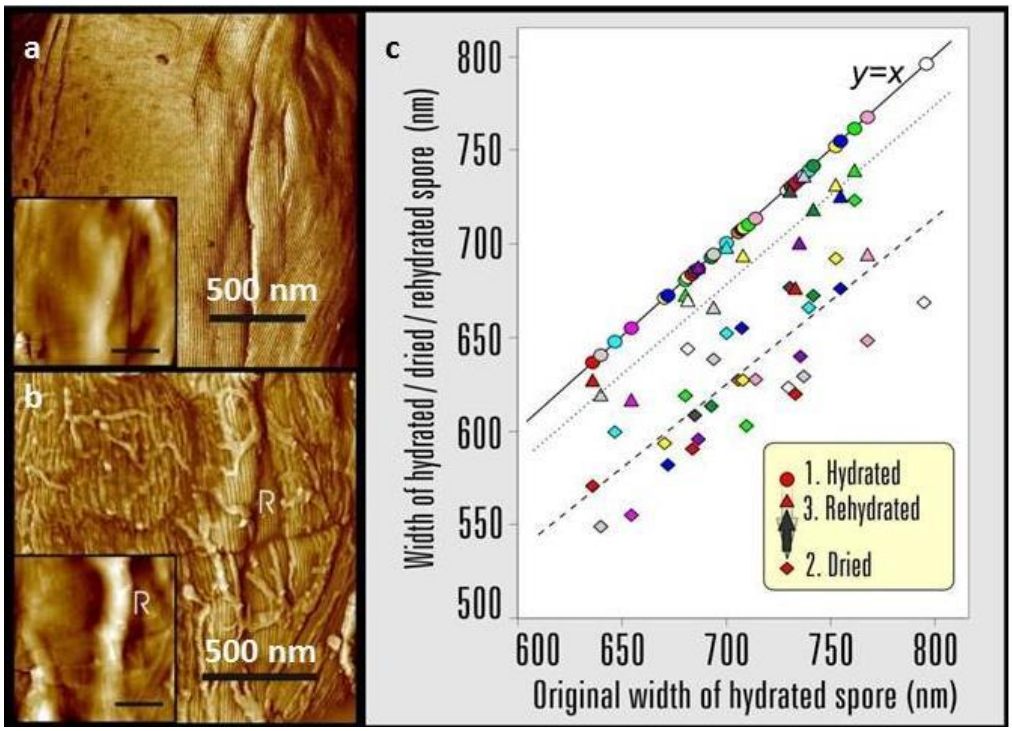

Figure 11. The effects of changing the *B.atrophaeus* spore environment from hydrated to dehydrated states, with AFM images showing (a) phase image and height image (inset) detail of a *B. atrophaeus* spore in water, showing rodlet spore coat structure and several shallow wrinkles, and (b) the same spore after drying, showing rodlet structure (with many adsorbed stray rodlets, which sedimented from the bulk solution upon drying of the sample) and a 60-nm high ridge (indicated with R). The graph (c) shows spore width variations of 35 individual *B. atrophaeus* spores, as a function of the size of the originally hydrated spore, followed by dehydration (24 hrs) (diamonds, dashed trend line), then rehydration (2 hours) (triangles, dotted trend line). For ease of comparison, the original hydrated spore width is (redundantly) depicted as circles, which by definition lie on the solid $y=x$ line. Thus, the three data points for one individual spore, depicted with the same color, are all on the same vertical line. Several spores detached from a substrate during rehydration experiments resulting in a smaller amount of experimental rehydration points (triangles). On average, spore size is reduced to 88% for dried spores, and returns to 97% of the original width for rehydrated spores. Images reproduced, with permission from Plomp et al., 2005a Copyright ©(2005) The Biophysical Society. Published by Elsevier, Inc.

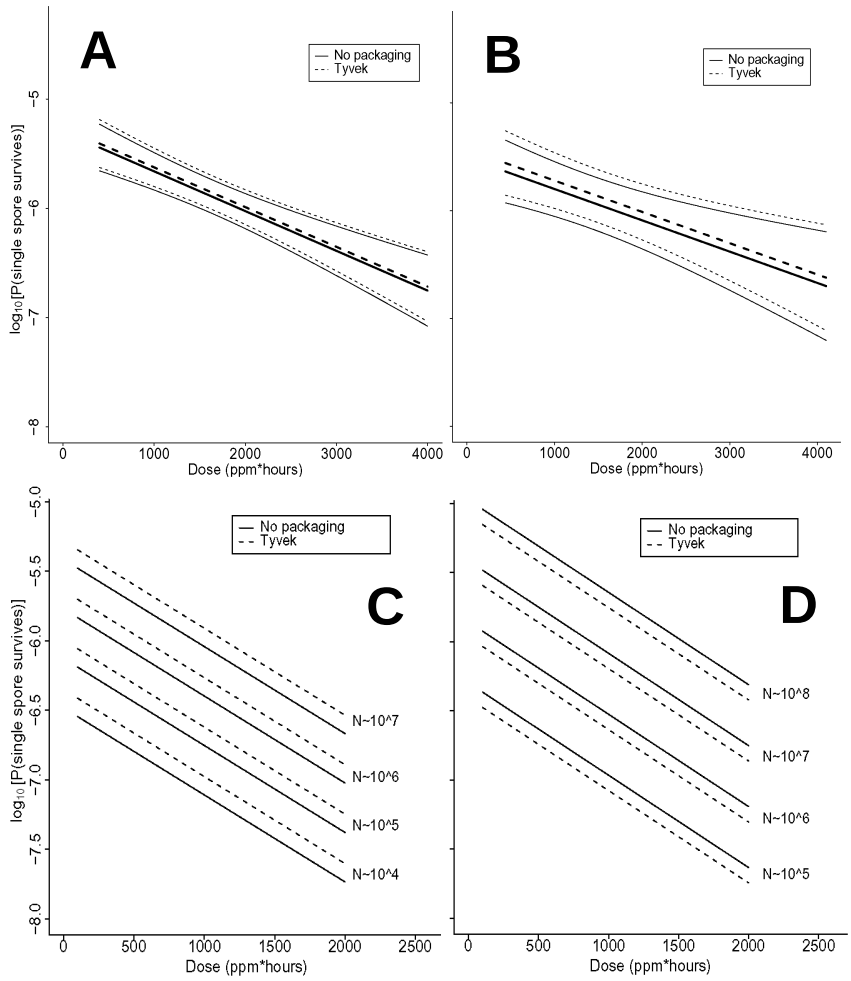

Figure 12A,B,C,D.
A) Statistical modeling showing the probability, with 95% confidence, of a single *B. thuringiensis* spore surviving a ClO_2 dose range of 438-4106 ppm-hours at 79% RH. The spore population of each strip is fixed at 1.2×10^6, and n = 98 each for strips contained in Tyvek or with no packaging. In the figure, the lighter set of dashed and solid lines represent the confidence interval for spore strips packaged in Tyvek or no packaging, respectively, while the middle bold lines represent the predicted probabilities. In this model, there is strong evidence of an effect of dose (*p = 0.002*) and no evidence of an effect of packaging (*p = 0.76*).

B) Statistical modeling showing the probability, with 95% confidence, of a single *G. stearothermophilus* spore surviving a ClO_2 dose range of 438-4106 ppm-hours at 79% RH. The spore population of each strip is fixed at 1.0×10^6, and n = 80 each for strips contained in Tyvek or no packaging. In the figure, the lighter set of dashed and solid lines represent the confidence interval for spore strips packaged in Tyvek or no packaging, respectively, while the middle bold lines represent the predicted probabilities. In this model, there is evidence of an effect of dose (*p = 0.02*) and no evidence of an effect of packaging (*p = 0.68*).

C) Predicted probabilities of a single spore surviving for varying numbers of *B. atrophaeus* spores (1.2×10^4 - 1.2×10^7), with a D_{EtO} value of 3.1, in Tyvek (n = 152) and no packaging (n = 144). Experiments were performed at 79% RH, and the ClO_2 dose ranged from 110-1991 ppm-hours. There is strong evidence that increased dose decreases the probability of any strips still having live spores ($p < 0.01$) and that as the number of spores on the strip increases, so does the probability of survival ($p < 0.01$). There is no evidence of a significant effect of packaging on survival of spores ($p = 0.21$), though there is some difference with a slightly higher rate of survival for spores packaged in Tyvek.

D) Predicted probabilities of a single spore surviving for varying numbers of *B. atrophaeus* spores (3.5×10^4 - 1.5×10^8), with a D_{EtO} value of 5.0, in Tyvek (n = 490) and no packaging (n = 350). Experiments were performed at 79% RH, and the ClO_2 dose ranged from 110-1991 ppm-hours. The results of this model exhibit similar behavior to Figure 2C, with the probability of a strip having live spores after treatment increasing with decreasing dose ($p < 0.01$) and with increasing numbers of spores ($p < 0.01$). Again there is no evidence of an effect of packaging ($p = 0.21$), but in this case there is a slightly lower rate of survival for spores in Tyvek packaging.

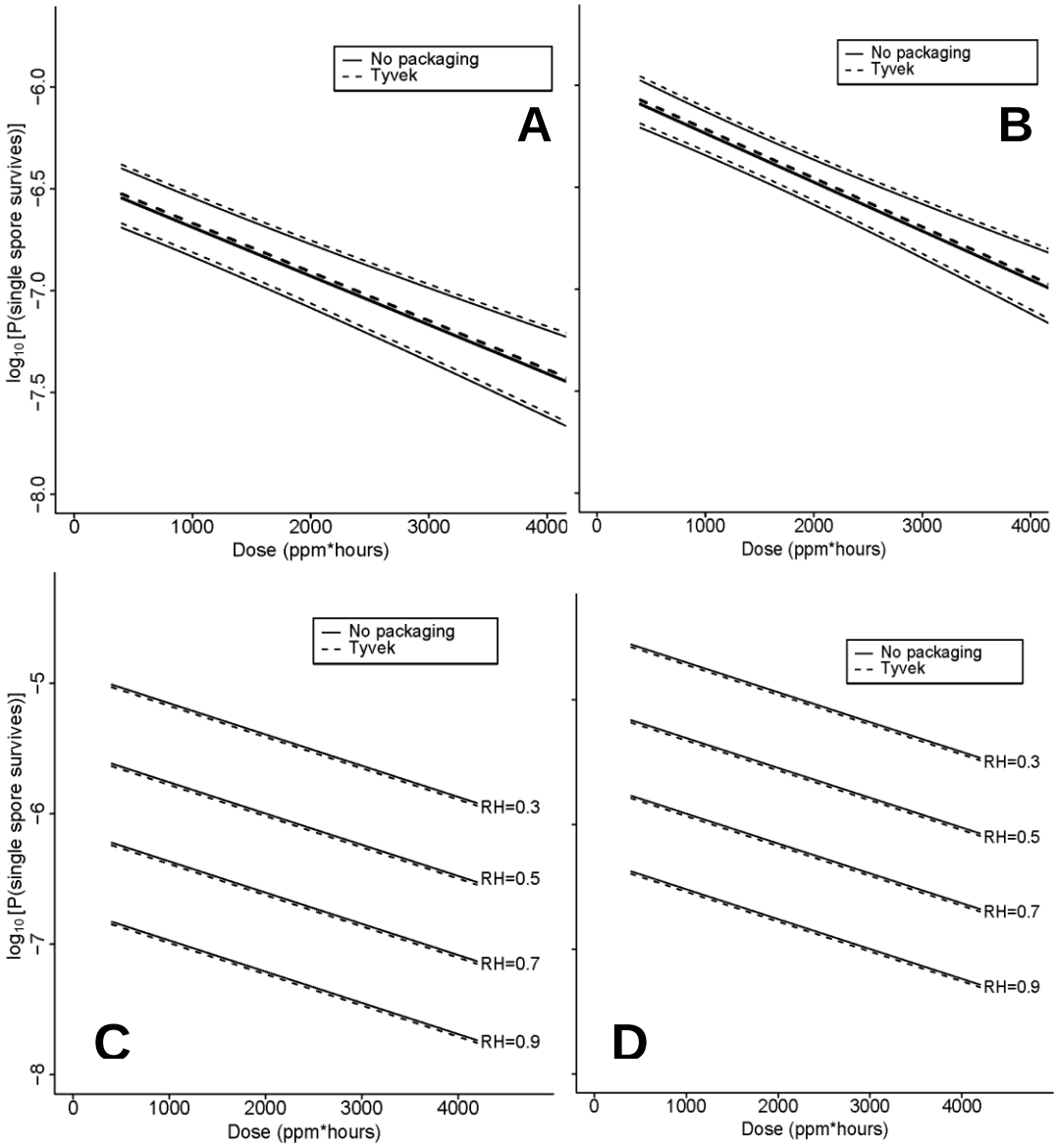

Figure 13A,B,C,D.
A) Statistical modeling showing the probability, with 95% confidence, of a single *B. atrophaeus* spore, with a D_{EtO} value of 3.1 and fixed strip inoculum of 10^6, in Tyvek (n = 38) and no packaging (n = 36), surviving a ClO_2 dose range of 110-199 ppm-hours at 79% RH. In the figures **A-D**, the lighter set of dashed and solid lines represent the confidence interval for spore strips packaged in Tyvek or no packaging, respectively, while the middle bold lines represent the predicted probabilities.

B) Statistical modeling showing the probability, with 95% confidence, of a single *B. atrophaeus* spore, with a D_{EtO} value of 5.0 and fixed strip inoculum of 10^6, in Tyvek (n = 98) and no packaging (n = 70), surviving a ClO_2 dose range of 110-1991 ppm-hours at 79% RH.

C) Predicted probabilities for a single *B. atrophaeus* spore, with a D_{EtO} value of 3.3 and fixed strip inoculum of 1.3×10^6, in Tyvek (n = 500, dashed line) or no packaging (n = 500, solid line).

D) with a D_{EtO} value of 3.8 and fixed strip inoculum of 1.3×10^6, in Tyvek (n = 498, dashed line) or no packaging (n = 498, solid line), surviving a range of ClO_2 doses with RH varying from 30%-90%. The results of this fitted model, which has an offset term of log(N) (fixed in this example) shows again that dose has a similarly strong effect as previously in that increasing it decreases the probability of spores surviving on a strip ($p < 0.01$). There is no evidence of an effect of packaging ($p = 0.73$), and there is strong evidence of an increase in survival probability with increasing D_{EtO} values ($p < 0.01$) and with decreasing RH ($p < 0.01$). The D_{EtO} variable was treated as a categorical variable to be consistent with earlier models and so the regression coefficient compares $D_{EtO} = 3.3$ to $D_{EtO} = 3.8$.

Figure 14 A,B,C,D.
A and B) Increasing RH at a fixed dose of (A) 500 ppm ClO_2 for 4 hours (~2000 ppm-hours) and (B) 1000 ppm ClO_2 for 4 hours (~4000 ppm-hours) results in a higher percentage of log 6 *B. atrophaeus* spore strips being killed. (A) ◆ = *B. atrophaeus* $D_{EtO} = 3.3$ (n = 120), □ = *B. atrophaeus* $D_{EtO} = 3.8$ (n = 160); (B) ◇ = *B. atrophaeus* $D_{EtO} = 3.3$ (n = 140), and ■ = *B. atrophaeus* $D_{EtO} = 3.8$ (n = 140). Data shown is for spore strips packaged in Tyvek. For the $D_{EtO} = 3.3$ strips exposed to ~2000 ppm-hours ClO_2, $\geq$ 80% kill is achieved at 70 %RH and above, but when we increase the dose to ~4000 ppm-hours the same level of kill is achieved at %RH of 60. The relationship between low D_{EtO} value and increased susceptibility to ClO_2 is evident, though, in this example, we see that at 90 %RH all four sample sets are behaving roughly the same.

C) *B. atrophaeus* $D_{EtO} = 3.3$, log 6 spore strips packaged in □ = medical-grade glassine, and ▨ = Tyvek are not equally susceptible to a set ClO_2 dose at 79 %RH (NE = no effect). Spore strips were exposed to 250 ppm ClO_2 for 4 hours (dose ≈ 1000 ppm-hours), where n = 20 each for glassine and Tyvek; 2000 ppm-hours, where n = 40 (glassine) and n = 20 (Tyvek); and 4000 ppm-hours, where n = 40 (glassine) and n = 20 (Tyvek) at constant temperature and %RH.

D) We did not achieve 100% kill for glassine-packaged log 6 spore strips until we subjected a lot of *B. atrophaeus* with D_{EtO} value of 3.0 (n = 20) to 2000 ppm for 10 hours (~20,000 ppm-hours) at 79 %RH. This high dose killed 80% and 85% of *B. atrophaeus* $D_{EtO} = 3.3$ and 3.8 (n = 20 each) spore strips, respectively.

E) For all three species and *B. atrophaeus* with two different D_{EtO} values (3.3, with n = 80 for each Tyvek and no packaging; and 3.8, with n = 189 for each Tyvek and no packaging), probabilities were predicted for a spore surviving after treatment, with RH = 0.79 and $N = 10^6$. Note that for *B. thuringiensis* (n = 98 each for Tyvek and no packaging), measurements were only made at $N = 1.2 \times 10^6$. For both sets of *B. atrophaeus*, measurements were made at $N = 1.3 \times 10^6$, so in these cases this plot involves extrapolation in *N*. *B. thuringiensis*, the closest phylogenetic relative to *B. anthracis* used in this study, is more likely to survive at any given

ClO_2 dose than either of the *B. atrophaeus* strains, though it's resistance is similar to the strain of *G. stearothermophilus* (n = 80 each for Tyvek and no packaging) assayed.

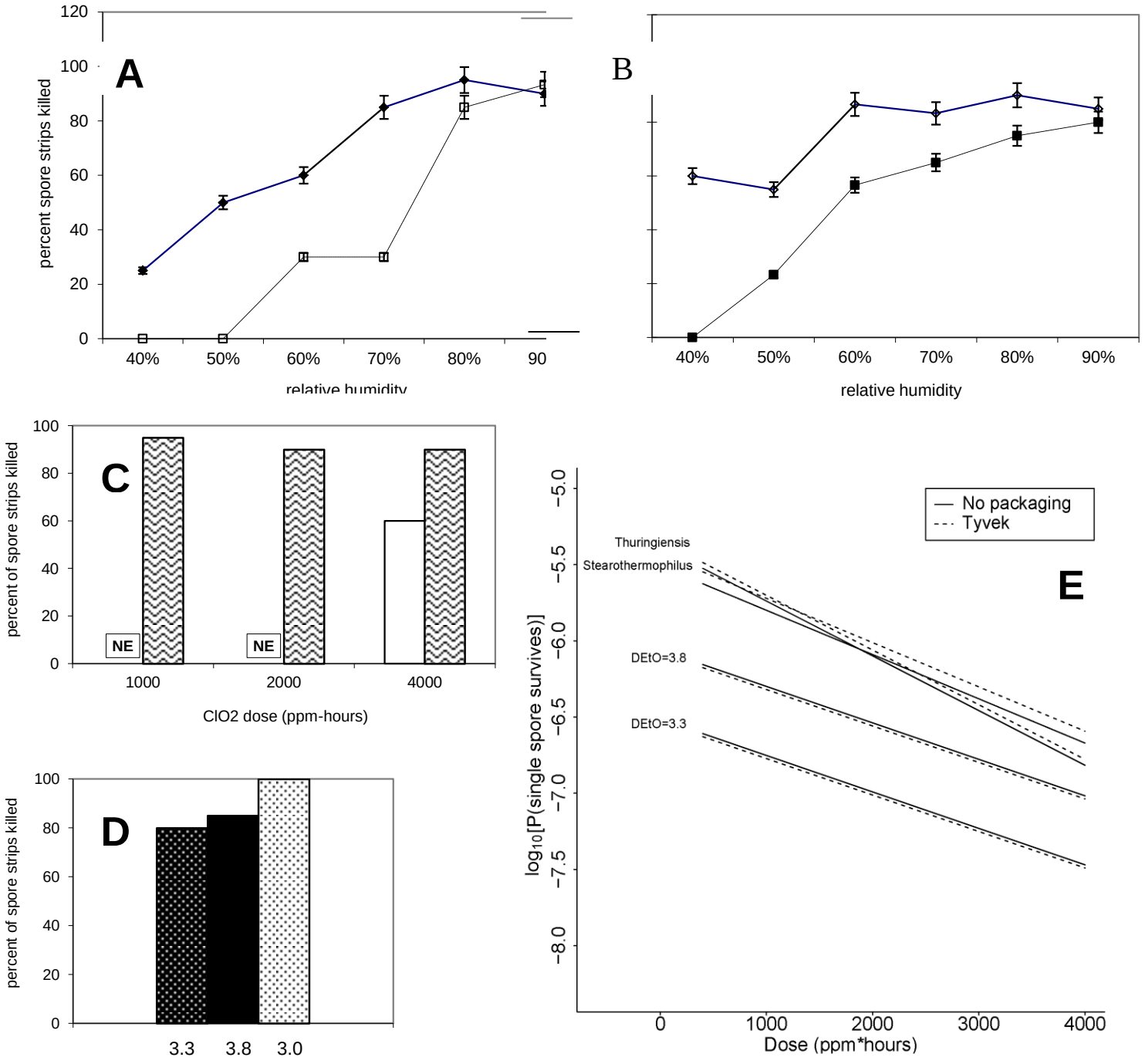

References

Aieta EM, Berg JD. 1986. A Review of Chlorine Dioxide in Drinking Water Treatment. *Journal of the American Water Works Association* 78(6), 62-72.

Anelich L, Moy GG. 2014 Ebola Virus Disease (EVD): Important aspects for the food science and technology community. IUFoST Scientific Information Bulletin (available at http://www.iufost.org/iufostftp/IUFoST%20SIB%20%20-%20Ebola%20Virus%20Disease%20update%201.pdf – accessed 12 March 2015).

Bruch CW. 1973. Sterilization of plastics: toxicity of ethylene oxide residues, p. 49-77. *In*: Industrial sterilization: International symposium (Phillips GB Miller WS, Eds.), Amsterdam, 1972. Duke University Press, Durham, N.C.

Buchanan CE, Neyman SL. 1986. Correlation of penicillin-binding protein composition with different functions of two membranes in *Bacillus subtilis* forespores. *Journal of Bacteriology*, 165, 498-503.

Burns DA, Heap JT, Minton NP. 2010. SleC is essential for germination of *Clostridium difficile* spores in nutrient-rich medium supplemented with the bile salt taurocholate. *Journal of Bacteriology* 192, 657-664.

Carroll AM, Plomp M, Malkin AJ, Setlow P. 2008. Protozoal digestion of coat-defective *Bacillus subtilis* spores produces "rinds" composed of insoluble coat protein. *Applied and Environmental Microbiology* 74, 5875-5881.

Chapman J, Lee W, Youkilis E, Martis L. 1986. Animal model for ethylene oxide (EtO) associated hypersensitivity reactions. *Transactions - American Society for Artificial Internal Organs* 32, 482-485.

Cléry-Barraud C, Gaubert A, Masson P, Vidal D. 2004. Combined Effects of High Hydrostatic Pressure and Temperature for Inactivation of *Bacillus anthracis* Spores. *Applied and Environmental Microbiology*, 70(1), 635-637. DOI: 10.1128/AEM.70.1.635-637.2004

Coleman WH, Chen D, Li Y-q, Cowan AE, Setlow P. 2007. How moist heat kills spores of *Bacillus subtilis*. *Journal of Bacteriology* 189, 8458-8466.

Coleman WH, Zhang P, Li Y-q, Setlow P. 2010. Mechanism of killing of spores of *Bacillus cereus* and *Bacillus megaterium* by wet heat. *Letters in Applied Microbiology* 50, 507-514.

Cortezzo DE, Koziol-Dube K, Setlow B, Setlow P. 2004. Treatment with oxidizing agents damages the inner membrane of spores of *Bacillus subtilis* and sensitizes spores to subsequent stress. *Journal of Applied Microbiology* 97, 838-852.

Cortezzo DE, Setlow P. 2004. Analysis of factors that influence the sensitivity of spores of *Bacillus subtilis* to DNA damaging chemicals. *Journal of Applied Microbiology* 98, 606-617.

Cowan AE, Koppel DE, Setlow B, Setlow P. 2003. A soluble protein is immobile in dormant spores of *Bacillus subtilis* but is mobile in germinated spores: implications for spore dormancy. *Proceedings of the National Academy of Sciences of the USA* 100, 4209-4214.

Cowan AE, Olivastro EM, Koppel DE, Loshon CA, Setlow B, Setlow P. 2004. Lipids in the inner membrane of dormant spores of *Bacillus* species are largely immobile. *Proceedings of the National Academy of Sciences of the USA* 101, 7733-7738.

Curtin MA, Dwyer S, Bukvic D, Doona CJ, Kustin K. 2014. Kinetics and mechanism of the reduction of sodium chlorite by sodium hydrogen ascorbate in aqueous solution at near neutral pH. *International Journal of Chemical Kinetics*, 46, 216-219.

Curtin MA, Taub IA, Kustin K, Sao N, Duvall JR, Davies KI, Doona CJ, Ross EW. 2004. Ascorbate-induced oxidation of formate by peroxodisulfate: product yields, kinetics, and mechanism. *Research on Chemical Intermediates*, 30(6), 647 661.

Cybulski RJ, Sanz P, Alem F, Stibitz S, Bull RL, O'Brien AD. 2009. Four superoxide dismutases contribute to *Bacillus anthracis* virulence and provide spores with redundant protection against oxidative stress. *Infection and Immunity* **77,** 271-285.

Dauphin LA, Newton BR, Rasmussen MV, Meyer RF, Bowen MD. 2008. Gamma irradiation can be used to inactivate *Bacillus anthracis* spores without compromising the sensitivity of diagnostic assays. *Applied and Environmental Microbiology* 74(14), 4427–4433.

Dolovich J, Marshall CP, Smith EKM, Shimizu A, Pearson FC, Sugona MA, Lee W. 1984. Allergy to ethylene oxide chronic hemodyalysis patients. *Artificial Organs* 8, 334-337.

Doona, C.J., Feeherry, F.E., Setlow, P., Malkin, A.J., Leighton, T.J. 2014. The Portable Chemical Sterilizer (PCS), D-FENS, and D-FEND ALL: Novel chlorine dioxide decontamination technologies for the military. *Journal of Visualized Experiments* (88), e4354 (available at http://www.jove.com/video/4354/the-portable-chemical-sterilizer-pcs-d-fens-d-fend-all-novel-chlorine, accessed 18 March 2015).

Driks A. 2003. The dynamic spore. *Proceedings of the National Academy of Sciences of the USA* 100, 3007–3009.

Driks A. 2009. The *Bacillus anthracis* spore. *Molecular Aspects of Medicine* 30, 368-373.

Elhadj S, Plomp M, Velsko SP, A.J. Malkin AJ. 2015. Assessment of the structural and morphological forensic signatures of single *Bacillus anthracis* spores (*in preparation*).

Foran A. 2013. NSRDEC patents help Army into 'Top 100 Global innovators' (available at http://www.army.mil/article/99816/ − accessed 12 March 2015).

Gerhardt P. 1967. Cytology of *Bacillus anthracis*. Federation Proceedings 26, 1504-1517.

Gerhardt P, Black SH. 1961. Permeability of bacterial spores. II. Molecular variables affecting solute permeation. *Journal of Bacteriology* 82, 750-760.

Gerhardt P, Marquis RE. 1989. Spore thermoresistance mechanisms, p. 43-63. *In*: Regulation of prokaryotic development (Smith I, Slepecky RA, and Setlow P, Eds.), American Society for Microbiology, Washington, DC.

Ghosh S, Setlow B, Wahome PG, Cowan AE, Plomp M. 2008. Characterization of spores of *Bacillus subtilis* that lack most coat layers. *Journal of Bacteriology* 190, 6741-6748.

Ghosal S, Leighton TJ, Wheeler KE, Hutcheon ID, Weber PK. 2010. Spatially-resolved characterization of water and ion incorporation in *Bacillus* spores. *Applied and Environmental Microbiology* 76, 3275-3282.

Griffiths K, Setlow P. 2009. Effects of modification of membrane lipid composition on *Bacillus subtilis* sporulation and spore properties. *Journal of Applied Microbiology* 106, 2064-2078.

Han Y, Floros JD, Linton RH, Nielsen SS, Nelson PE. 2001. Response surface modeling for the inactivation of *Escherichia coli* O157:H7 on green peppers (*Capsicum annuum* L.) by chlorine dioxide gas treatments. *Journal of Food Protection* 64(8), 1128-1131.

Han Y, Guentert AM, Smith RS, Linton RH, Nelson PE. 1999. Efficacy of chlorine dioxide gas as a sanitizer for tanks used for aseptic juice storage. *Food Microbiology* 16, 53-61.

Hayes CS, Setlow P. 2001. An α/β-type small, acid-soluble spore protein which has a very high affinity for DNA prevents outgrowth of *Bacillus subtilis* spores. *Journal of Bacteriology* 183, 2662-2666.

Henriques AO, Moran CP. 2007. Structure, assembly, and function of the spore surface layers. *Annual Reviews in Microbiology* 61, 555-588.

Horváth AK, Nagypál I, Peintler G, Epstein IR, Kustin K. 2003. Kinetics and mechanism of the decomposition of chlorous acid. *Journal of Physical Chemistry A, 107,* 6966-6973.

Illades-Aguiar B, Setlow P. 1994. Autoprocessing of the protease that degrades small, acid-soluble proteins of spores of *Bacillus* species is triggered by low pH, dehydration and dipicolinic acid. *Journal of Bacteriology* 176, 7032-7037.

Kaieda S, Setlow B, Setlow P, Halle B. 2013. Mobility of core water in *Bacillus subtilis* spores by ^{2}H NMR. *Biophysics Journal* 105, 2016-2023.

Klämpfl TG, Isbary G, Shimizu T, Li Y-F, Zimmerman JL, Stolz W, Schlegl J, Morfill GE, Schmidt H-U. 2012. Cold atmospheric plasma and plasma sterilization against spores and other microorganisms of interest. *Applied and Environmental Microbiology* 78, 5077-5082.

Kong L, Doona CJ, Setlow P, Li Y-q. 2014. Monitoring rates and heterogeneity of high pressure germination of *Bacillus* spores using phase contrast microscopy of individual spores. *Applied and Environmental Microbiology* 80, 345-353.

Kong L, Setlow P, Li Y-q. 2013. Direct analysis of water content and movement in single dormant bacterial spores using confocal Raman microspectroscopy. *Analytical Chemistry* 85, 7094-7101.

Lee KS, Bumbaca D, Kosman J, Setlow P, Jedrzejas MJ. 2008. Structure of a protein-DNA complex essential for DNA protection in spores of *Bacillus* species. *Proceedings of the National Academy of Sciences of the USA* 105, 2806-2811.

Leggett, M, McDonnell G, Denyer S, Setlow P, Maillard J-Y. 2012. Bacterial spore structures and their protective role in biocide resistance. *Journal of Applied Microbiology* 113, 485-499.

Lettman SF, Boltansky H, Alter HJ, Pearson FC, Kaliner MA. 1986. Allergic reaction in healthy plateletpheresis donors caused by sensitization to ethylene oxide gas. *New England Journal of Medicine* 315, 1192-1196.

Luu S, Cruz-Mora J, Setlow B, Feeherry FE, Doona CJ, Setlow P. 2015. The effects of heat activation on *Bacillus* spore germination, with nutrients or under high-pressure, with and without germination proteins. *Applied and Environmental Microbiology* (*in press*).

Lykins BW, Koffskey WE, Patterson KS. 1994. Alternative disinfectants for drinking water treatment. *Journal of Environmental Engineering* 120, 745-758.

Malkin AJ. 2011. Resolving the high-resolution architecture, assembly and functional repertoire of bacterial systems by *in vitro* atomic force microscopy. *In*: Life at the Nanoscale: Atomic Force Microscopy of Live Cells (Dufresne Y, Ed.). Pan Stanford Publishing. Singapore, ISBN 978-981-4267-96-0, pp. 71-99.

Malkin AJ, Plomp M. 2010. High-resolution architecture and structural dynamics of microbial and cellular system: Insights from high-resolution *in vitro* atomic force microscopy. *In*: Scanning Probe Microscopy of Functional Materials: Nanoscale Imaging and Spectroscopy (Kalinin SV, Gruverman A, Eds.). New York: Springer. pp. 39-68.

Margosch D, Ehrmann MA, Gänzle MG, Vogel RF. 2004. Comparison of pressure and heat resistance of *Clostridium botulinum* and other endospores in mashed carrots. *Journal of Food Protection* 67, 2530-2537.

McKenney PT, Driks A, Eichenberger P. 2013. The *Bacillus subtilis* endoscpore and functions of the multilayered coat. *Nature Reviews Microbiology* 11, 33-44. DOI: 10.1038/nrmicro2921. Epub 2012 Dec 3.

Moeller R, Raguse M, Reitz G, Okayasu R, Li Z, Klein S, Setlow P, Nicholson WL. 2014. Resistance of *Bacillus subtilis* spore DNA to lethal ionizing radiation damage relies primarily on

spore core components and DNA repair, with minor effects of oxygen radical detoxification. *Applied and Environmental Microbiology* 80, 104-109.

Muttamara S, Sales CI, Gazali Z. 1995. The formation of trihalomethane from chemical disinfectants and humic substances in drinking water. *Water Supply* 13(2), 105-117.

Paidhungat M, Setlow B, Driks A, Setlow P. 2000. Characterization of spores of *Bacillus subtilis* which lack dipicolinic acid. *Journal of Bacteriology* 182, 5505-5512.

Paredes-Sabja D, Setlow P, Sarker MR. 2009a. The protease CspB is essential for initiation of cortex hydrolysis and DPA release during germination of spores of *Clostridium perfringens*. *Microbiology* 155, 3464-3472.

Paredes-Sabja D, Setlow P, Sarker MR. 2009b. SleC is essential for cortex peptidoglycan hydrolysis during germination of spores of the pathogenic bacterium *Clostridium perfringens*. *Journal of Bacteriology* 191, 2711-2720.

Plomp M, Leighton TJ, Wheeler KE, Malkin AJ. 2005a. The high-resolution architecture and structural dynamics of *Bacillus* spores. *Biophysical Journal* 88, 603-608.

Plomp M, Leighton TJ, Wheeler KE, Malkin AJ. 2005b. Architecture and high-resolution structure of *Bacillus thuringiensis* and *Bacillus cereus* spore coat surfaces. *Langmuir* 21, 7892-7898.

Plomp M, Leighton TJ, Wheeler KE, Pitesky ME, Malkin AJ. 2005c. *Bacillus atrophaeus* outer spore coat assembly and ultrastructure. *Langmuir* 21, 10710-10716.

Plomp M, Leighton TJ, Wheeler KE, Hill HD, Malkin AJ. 2007a. *In vitro* high-resolution structural dynamics of single germinating bacterial spores. *Proceedings of the National Academy of Sciences of the USA* 104, 9644-9649.

Plomp M, Malkin AJ. 2009. Mapping of proteomic composition on the surfaces of *Bacillus* spores by atomic force microscopy. *Langmuir* 25, 403-409.

Plomp M, Monroe C, Setlow P, Malkin AJ. 2014. Architecture and assembly of the *Bacillus subtilis* spore coat. PLoS ONE 9; e108560.

Plomp M, McCaffery JM, Cheong I, Huang X, Bettegowda C. 2007b. Spore coat architecture of *Clostridium novyi* NT spores. *Journal of Bacteriology* 189, 6457-6468.

Popham DL. 2002. Specialized peptidoglycan of the bacterial endospore: the inner wall of the lockbox. *Cellular and Molecular Life Sciences* 59, 426-433.

Reineke K, Mathys A, Heinz V, Knorr D. 2013a. Mechanisms of endospore inactivation under high pressure. *Trends in Microbiology* 21, 296-304.

Reineke K, Schlumbach K, Baier D, Mathys A, Knorr D. 2013b. The release of dipicolinic acid – the rate-limiting step of *Bacillus* endospore inactivation during the high pressure thermal sterilization process. *International Journal of Food Microbiology* 162, 55-63.

Rode LJ, Lewis CW, Foster JW. 1962. Electron microscopy of spores of *Bacillus megaterium* with special emphasis to the effects of fixation and thin sectioning. *Journal of Cellular Biology* 13, 423-435.

Rosenblatt DH, Rosenblatt AA, Knapp JA. 1987. Use of chlorine dioxide gas as a chemosterilizing agent. US patent# 4681739, 21 July 1987).

Roth S, Feichtinger J, Hertel C. 2010. Characterization of *Bacillus subtilis* spore inactivation in low-pressure, low temperature gas plasma sterilization processes. *Journal of Applied Microbiology* 108, 521-531.

Setlow B, Loshon CA, Genest PC, Cowan AE, Setlow C, Setlow P. 2002. Mechanisms of killing of spores of *Bacillus subtilis* by acid, alkali and ethanol. *Journal of Applied Microbiology* 92, 362-375.

Setlow B, Parish S, Zhang P, Li Y-q, Neely WC, Setlow P. 2014. Mechanism of killing of spores of *Bacillus anthracis* in a high temperature gas environment *Journal of Applied Microbiology* 116, 805-14.

Setlow B, Setlow P. 1980. Measurements of the pH within dormant and germinated spores of *Bacillus megaterium*. *Proceedings of the National Academy of Sciences of the USA* 77, 2744-2746.

Setlow P. 1994. Mechanisms which contribute to the long-term survival of spores of *Bacillus* species. *Journal of Applied Bacteriology* 76, 49S-60S.

Setlow P. 2001. Resistance of spores of *Bacillus* species to ultraviolet light. *Environmental and Molecular Mutagenesis* 38, 97-104.

Setlow P. 2006. Spores of *Bacillus subtilis*: their resistance to radiation, heat and chemicals. *Journal of Applied Microbiology* 101, 514-525.

Setlow P. 2007. Germination of spores of *Bacillus subtilis* by high pressure. *In*: High Pressure Processing of Foods (Doona CJ and Feeherry FE, Eds.), pp. 15-40. Blackwell Publishing, London.

Setlow P. 2007. I will survive: DNA protection in bacterial spores. *Trends in Microbiology* 15, 172-180.

Setlow P. 2013. When the sleepers wake: the germination of bacterial spores. *Journal of Applied Microbiology* 115, 1251-1268.

Setlow P, Doona CJ, Feeherry FE, Kustin K, Sisson D, Chandra S. 2009. Enhanced safety and extended shelf-life of fresh produce for the military. *In*: Microbial Safety of Fresh Produce (Fan X, Niemira BA, Doona CJ, Feeherry FE, Gravani RB, Eds.). IFT Press/Wiley-Blackwell, Ames, IA, pp 263-289.

Setlow P, Johnson EA. 2012. Spores and their significance, p. 45-79. *In*: Food microbiology: fundamentals and frontiers, 4th ed. (Doyle MP, Buchanan R, Eds.), ASM Press, Washington, DC.

Setlow P, Liu J, Faeder JR. 2012. Heterogeneity in bacterial spore populations, p. 201-216. *In*: Bacterial Spores: Current Research and Applications (Abel-Santos E, Ed.) Horizon Scientific Press, Norwich, UK.

Sevenich R, Kleinstueck E, Crews C, Anderson W, Pye C, Riddellova K, Hradecky J, Moravcova E, Reineke K, Knorr D. 2014. High-pressure thermal sterilization: food safety and food quality of baby food purée. *Journal of Food Science* 79, M230-7.

Simpson GD, Miller RF, Laxton GD, Clements WR. 1993. A focus on chlorine dioxide: the "ideal" biocide. Corrosion 93, New Orleans, LA, 8-12 March 1993, paper no. 472 (available at http://www.clo2.gr/en/pdf/secure/chlorinedioxideidealbiocide.pdf, accessed 18 March 2015).

Stubblefield JM, Newsome AL. 2015. Potential biodefense model applications for portable chlorine dioxide gas production. *Health Security*, 13(1); DOI: 10.1089/hs.2014.0017.

Sunde EP, Setlow P, Hederstedt L, Halle B. 2009. The physical state of water in bacterial spores. *Proceedings of the National Academy of Sciences of the USA* 106, 19334-19339.

Swerdlow BM, Setlow B, Setlow P. 1981. Levels of H^+ and other monovalent cations in dormant and germinating spores of *Bacillus megaterium*. *Journal of Bacteriology* 148(1), 20-29.

van Bokhorst-van de Veen H, Xie H, Esveld E, Abee T, Mastwijk H, Groot MN. 2015. Inactivation of chemical and heat-resistant spores of *Bacillus* and *Geobacillus* by nitrogen cold atmospheric plasma evokes distinct changes in morphology and integrity of spores. *Food Microbiology* 45, 26-33.

Westphal AJ, Price PB, Leighton TJ, Wheeler KE. 2003. Kinetics of size changes of individual *Bacillus thuringiensis* spores in response to changes in relative humidity. *Proceedings of the National Academy of Sciences of the USA* 100, 3461–3466.

World Health Organization (WHO). 2014. Ebola virus disease (available at http://www.who.int/mediacentre/factsheets/fs103/en/ − accessed 12 March 2015).

World Health Organization (WHO). 2015. The Five Keys to Safer Food Programme (available at http://www.who.int/mediacentre/factsheets/fs103/en/ − accessed 12 March 2015).

Yardimci O, Setlow P. 2010. Plasma sterilization: Opportunities and microbial assessment strategies in medical device manufacturing. *IEEE Transactions on Plasma Sciences* 38, 973-981.

Zhang P, Thomas S, Li Y-q, Setlow P. 2012. Effects of cortex peptidoglycan structure and cortex hydrolysis on the kinetics of Ca^{2+}-dipicolinic acid release during *Bacillus subtilis* spore germination. *Journal of Bacteriology* 194, 646-652.